



^{207}Pb - ^{206}Pb , ^{40}Ar - ^{39}Ar and Fission-Track Geothermochronology Quantifying Cooling and Exhumation History of the Kaman-Kırşehir Region Intrusions, Central Anatolia, Turkey

DURMUŞ BOZTUĞ¹, ÖZLEM GÜNEY², MATT HEIZLER³, RAYMOND C. JONCKHEERE⁴,
MARION TICHOMIROWA⁵ & NAZMİ OTLU²

¹ Faculty of Engineering, University of Tunceli, TR-62000 Tunceli, Turkey

(E-mail:boztug@cumhuriyet.edu.tr)

² Department of Geological Engineering, Cumhuriyet University, TR-58140 Sivas, Turkey

³ New Mexico Bureau of Geology and Mineral Resources, New Mexico Technology, 801 Leroy Place, Socorro, NM 87801, USA

⁴ Geologisches Institut, TU Bergakademie Freiberg, Bernhard-von-Cottastraße 2, D-09599 Freiberg, Germany

⁵ Mineralogisches Institut, TU Bergakademie Freiberg, Brennhausgasse 14, D-09596 Freiberg, Germany

Received 01 April 2007; revised typescript received 27 November 2007; accepted 05 February 2008

Abstract: The Kaman-Kırşehir region intrusions were generated in a post-collisional extensional setting following Cenomanian-Turonian docking of an oceanic island arc, comprising the supra-subduction zone (SSZ) Central Anatolian ophiolite (CAO), onto the Tauride-Anatolide Platform (TAP). These granitoids have been named, from N to S, the Çamsarı quartz syenite, Hamit quartz syenite, Bayındır nepheline-cancrinite syenite, Durmuşlu nepheline-nosean-melanite syenite porphyry and Baranadağ quartz monzonite. They intrude the crustal metasediments of the Central Anatolian Crystalline Complex (CACC) and CAO and are unconformably overlain by Upper Paleocene to Lower-Middle Eocene sediments.

The single-zircon ^{207}Pb - ^{206}Pb evaporation age of the Çamsarı unit is 95.7 ± 5.1 Ma; those of the Hamit and Baranadağ units are indistinguishable with a weighted mean of 74.3 ± 4.5 Ma. The amphibole ^{40}Ar - ^{39}Ar ages of the Hamit and Baranadağ units are almost identical with a weighted mean of 72.7 ± 0.1 Ma. The apatite fission-track age vs elevation plot for the Çamsarı, Hamit, Durmuşlu and Baranadağ samples reveals rapid exhumation (>1 km/Ma) between ~ 57 and ~ 61 Ma, consistent with the results of track-length modelling. This Early–Middle Paleocene rapid exhumation is thought to result from uplift triggered by continent (TAP) – continent (Eurasian plate; EP) collision following the closure of İzmir-Ankara-Erzincan (İAE) ocean that also initiated the formation of peripheral foreland basins in central Anatolia.

Key Words: single zircon ^{207}Pb - ^{206}Pb , amphibole ^{40}Ar - ^{39}Ar , apatite fission-track, cooling, exhumation, Kaman-Kırşehir region, central Anatolia, Turkey

Kaman-Kırşehir Yöreni İträzyonlarının ^{207}Pb - ^{206}Pb , ^{40}Ar - ^{39}Ar ve Fizyon İzi Jeotermokronolojisi Yöntemleriyle Soğuma ve Yüzeyleme Tarihçelerinin Belirlenmesi, Orta Anadolu, Türkiye

Özet: Kaman-Kırşehir yöreni granitik intrüzyonları, Torid-Anatolid platformu (TAP) ve yitim zonu üzerinde gelişen Orta Anadolu Ofiyolitini (OAO) içeren okyanusal ada yayı arasında Senomaniyen–Türoniyen’de gerçekleşen kita-okyanusal ada yayı çarpışması sonrası gerilme rejiminde oluşmuşlardır. Bu granitoyidler, kuzeyden güneye doğru, Çamsarı kuvars siyeniti, Hamit kuvars siyeniti, Bayındır nefelin-kankrinit siyeniti, Durmuşlu nefelin-nozeyan-melanit siyenit porfiri ve Baranadağ kuvars monzoniti birimlerinden oluşur. Bu intrüzif kayaçlar, Orta Anadolu Kristalin Karmaşığına (OAKK) ait metamorfik kayaçlarla OAO’ne ait birimleri sıcak dokanakla keser ve Geç Paleosen–Erken/Orta Eosen yaşılı sedimanter birimler tarafından uyumsuz olarak örtülürler.

Çamsarı kuvars siyenitinin tek zirkon ^{207}Pb - ^{206}Pb buharlaşma yaşı 95.7 ± 5.1 My olarak bulunmuştur; Hamit ve Baranadağ birimlerinin yaşıları ise birbirlerinden ayırt edilemeyecek derecede yakın olup, ağırlıklı ortalaması yaşı 74.3 ± 4.5 My olarak belirlenmiştir. Benzer şekilde, Hamit ve Baranadağ birimlerinin amfibol ^{40}Ar - ^{39}Ar yaşıları da birbirlerinden ayırt edilemeyecek derecede yakındır ve ağırlıklı ortalaması yaşı 72.7 ± 0.1 My olarak belirlenmiştir. Çamsarı, Hamit, Baranadağ ve Durmuşlu birimlerinin apatit fizyon izi yaş verilerinin (deniz düzeyinden) yükseliş eğilimleri incelenince, ~ 57 ve ~ 61 My aralığında oldukça hızlı bir yükselme hızıyla (> 1 km/My) yüzeyleme tarihçesi, aynı zamanda, fizyon izi uzunluk ölçümüne dayalı zaman-sıcaklık modelleme çalışmalarıyla da desteklenmiştir. Apatit fizyon izi jeotermokronolojisi verileriyle belirlenen Erken–Orta Paleosen yaşı bu hızlı yüzeylemenin, İzmir-Ankara-Erzincan (İAE) okyanusunun kapanmasını takiben TAP ve Avrasya Levhası (AL) arasında gelişen kita-kita çarpışmasına bağlı sıkışma rejimiyle meydana geldiği ve hatta bu sırada Orta Anadolu önde basenlerinin de (OAÖB) açıldığı ileri sürülmektedir.

Anahtar Sözcükler: tek zirkon ^{207}Pb - ^{206}Pb , amfibol ^{40}Ar - ^{39}Ar , apatit fizyon izi, tektonik yüzeyleme, soğuma tarihçesi, Kaman-Kırşehir intrüzyfleri, Orta Anadolu, Türkiye

Introduction

Most geochemical and petrogenetic studies of the Central Anatolian Granitoids (CAG; Figure 1) place them in a post-collisional setting, related to the evolution of the Izmir-Ankara-Erzincan ocean, a strand of the northern Neo-Tethys (Akıman *et al.* 1993; Erler & Göncüoğlu 1996; Boztuğ 1998, 2000; Düzgören-Aydın *et al.* 2001; Köksal *et al.* 2001, 2004; İlbeli *et al.* 2004; İlbeli 2005; Boztuğ & Arehart 2007; Köksal & Göncüoğlu 2008). Kadioğlu *et al.* (2003), in contrast, proposed an Andean type arc-related setting for the Ağaçören intrusive suite from the western part of the Central Anatolian Granitoids. Boztuğ *et al.* (2007a, b) and Boztuğ & Jonckheere (2007) reported that collision occurred during Cenomanian–Turonian time between the Tauride-Anatolide Platform (TAP) and an intra-oceanic island arc, comprising the supra-subduction zone (SSZ) type central Anatolian ophiolites (CAO).

Geochronological studies of the CAG can be subdivided into three groups on the basis of the closure temperatures (T_c ; Dodson 1973, 1979) of the radiometric system: (1) high- T_c methods, giving intrusion ages (Ataman 1972; Göncüoğlu 1986; Gündoğdu *et al.* 1988; Zeck & Ünlü 1988; Kuruç 1990; Güleç 1994; Whitney *et al.* 2003; Köksal *et al.* 2004; Boztuğ *et al.* 2007b); (2) medium- T_c methods, giving cooling ages (Göncüoğlu 1986; Yalınız *et al.* 1999; Whitney *et al.* 2003; Kadioğlu *et al.* 2003; İlbeli *et al.* 2004; Tatar & Boztuğ 2005; Önal *et al.* 2005; Boztuğ & Harlavan 2008; Boztuğ *et al.* 2007a) and (3) low- T_c methods, giving exhumation ages (Fayon *et al.* 2001; Boztuğ & Jonckheere 2007; Fayon & Whitney 2007). These studies indicate an intrusion period ranging from early Late Cretaceous (Cenomanian–Turonian) to Campanian, a cooling period from the Campanian to the Maastrichtian and an exhumation period from the Paleocene through the Oligocene to the Miocene.

The present investigation aims to put age constraints on the emplacement, cooling and exhumation of the Kaman-Kırşehir-region intrusions (Figures 1 & 2) based on new single-zircon ^{207}Pb - ^{206}Pb evaporation ages, hornblende ^{40}Ar - ^{39}Ar ages and apatite fission-track ages supplemented with track-length data.

Geological Background

The mineralogical-petrographical and whole-rock geochemical characteristics of the intrusive rocks were

previously reported by Otlu & Boztuğ (1998). The crustal metasediments of the Central Anatolian Crystalline Complex (CACC) surrounding the Baranadağ and Kortundağ intrusions in the Kırşehir-Kaman region underwent medium-P (6–7 kbar), high-T (700–750 °C) regional metamorphism (Whitney *et al.* 2001) about 84.1 ± 0.8 Ma ago (monazite U-Pb SHRIMP age; Whitney & Hamilton 2004). The basement, comprising the CAG, CACC and the Central Anatolian Ophiolite (CAO; Yalınız *et al.* 1996, 2000; Floyd *et al.* 2000), is unconformably overlain by the Middle Eocene Baraklı and Mio–Pliocene Kızılırmak formations (Figure 2). There are some geothermochronologic studies which were carried out in the Kaman-Kırşehir-region intrusions by various authors. For example, Gündoğdu *et al.* (1988) reported a Rb-Sr whole-rock isochron age of 70.7 ± 1.1 Ma for the Bayındır granitoid, while Kuruç (1990) reported Rb-Sr whole-rock isochron ages ranging from 85.1 ± 3.6 to 70.5 ± 3.4 Ma for the same granitoid unit. Köksal *et al.* (2004) determined titanite U-Pb ages of 74.1 ± 0.7 Ma and 74.0 ± 2.8 Ma for the Çamsarı quartz syenite and Baranadağ quartz monzonite, respectively. Apart from these crystallization ages based on high-T geothermochronometry methods mentioned above, there are also some K-Ar and Ar-Ar cooling age data for the Kaman-Kırşehir region intrusive rocks. İlbeli *et al.* (2004) reported a hornblende K-Ar cooling age of 76.4 ± 1.3 Ma for the Baranadağ and a biotite K-Ar cooling age of 66.6 ± 1.1 Ma for the Cefalıdağ granitoid in the Kaman-Kırşehir region. Kadioğlu *et al.* (2006) have also performed Ar-Ar dating on the amphibole and biotite separates from the Cefalıdağ granitoid which yielded cooling ages of 70.9 ± 0.2 and 70.8 ± 0.4 to 71.0 ± 0.4 Ma, respectively. Similar amphibole and biotite Ar-Ar cooling ages were obtained from the Bayındır nepheline syenite by Kadioğlu *et al.* (2006), amphiboles giving an age of 69.2 ± 0.7 to 70.1 ± 0.4 Ma, while biotites yielding an age of 70.3 ± 0.2 Ma.

The intrusive rocks in the Kaman-Kırşehir region are simply divided into two groups: (1) the Baranadağ quartz monzonite unit in the south and (2) the Kortundağ intrusions in the north, comprising the Hamit quartz syenite, Çamsarı quartz syenite, Bayındır nepheline-cancrinite syenite and Durmuşlu nepheline-nosean-melanite syenite porphyry units. Their emplacement age is Late Cretaceous to Early Eocene in the light of regional correlations combined with biostratigraphic age data from the Baraklı formation. The principal mineralogical-

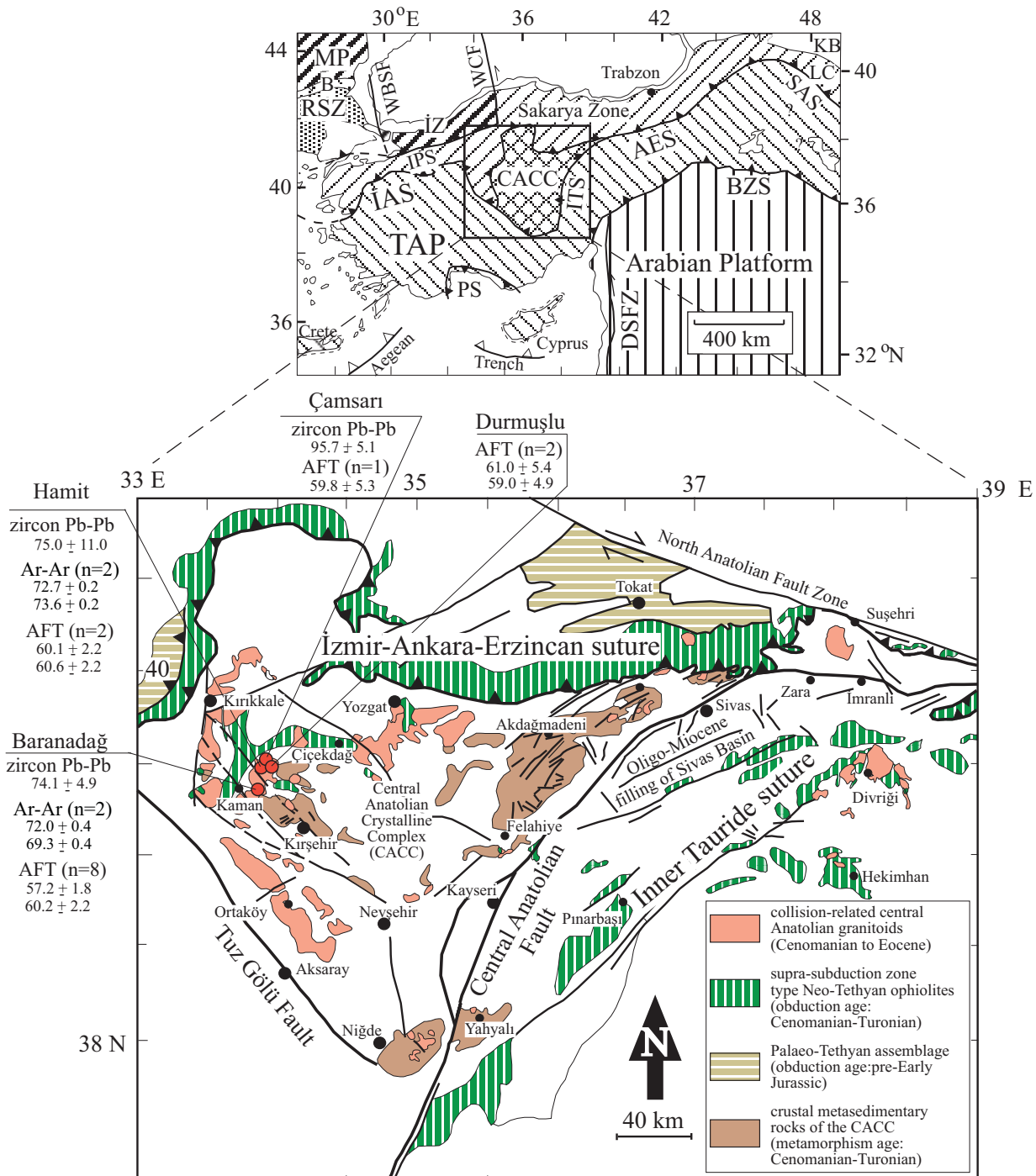


Figure 1. Regional geological setting of the Kaman-Kırşehir region intrusions in central Anatolia (modified after Boztuğ & Jonckheere 2007). Upper inset modified after Okay & Tüysüz (1999). Abbreviations in upper inset are as follow: MP- Moesian Platform, B- Balkanides, RSZ- Rhodope-Strandja Zone, WBSF- West Black Sea Fault, WCF- West Crimean Fault, İZ- İstanbul Zone, IPS- Intra-Pontide Suture, İAS- İzmir-Ankara Suture, CACC- Central Anatolian Crystalline Complex, PS- Pamphylian Suture, ITS- Inner Tauride Suture, AES- Ankara-Erzincan Suture, DSFZ- Dead Sea Fault Zone, KB- Kura Basin, LC- Lesser Caucasus, SAS- Sevan-Akera Suture, BZS- Bitlis-Zagros Suture, TAP- Tauride-Anatolide Platform.

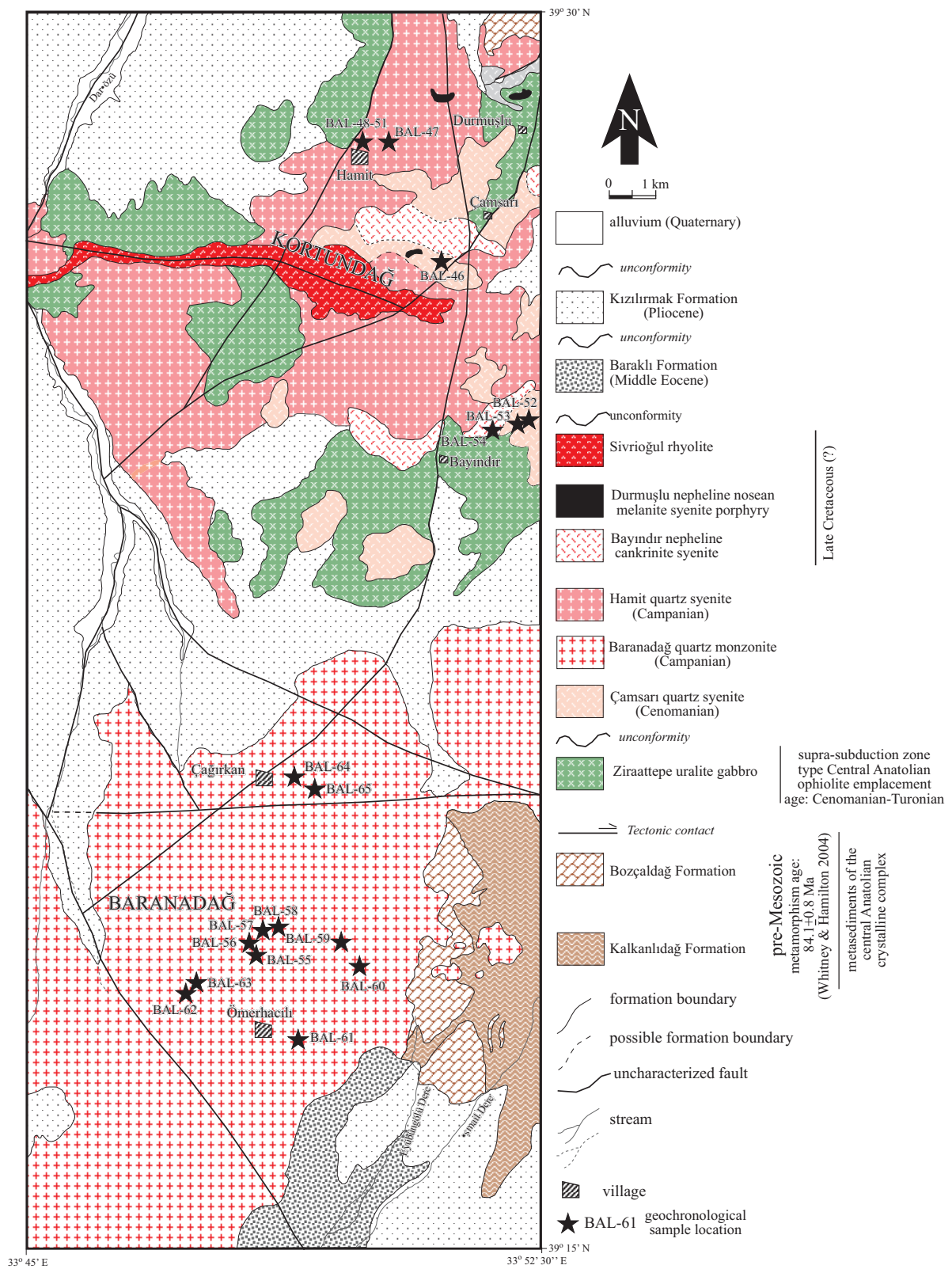


Figure 2. Geological map of the Kaman-Kırşehir region intrusions (revised from Otlu & Boztuğ 1998).

petrographical characteristics of the Baranadağ, Hamit, Çamsarı and Durmuşlu units are as follows:

Baranadağ Quartz Monzonite and Hamit Quartz Syenite

The Baranadağ quartz monzonite and Hamit quartz syenite are porphyritic with K-feldspar megacrysts set in a medium- to coarse-grained groundmass consisting of plagioclase, K-feldspar (orthoclase, perthite, microcline), hastingsitic amphibole, augitic pyroxene, biotite and quartz. The accessory minerals are titanite, apatite, zircon, allanite and opaque oxides. The difference between the Baranadağ and Hamit units is that the former contains more plagioclase than K-feldspar.

Çamsarı Quartz Syenite

This unit presents a medium-grained equigranular texture. The major rock-forming minerals are K-feldspar (orthoclase+perthite), plagioclase, hastingsitic amphibole, biotite, quartz and fluorite, whereas the accessory constituents consist of titanite, xenotime, apatite, zircon and opaque minerals.

Durmuşlu Nepheline-Nosean-Melanite Syenite Porphyry

This unit is exposed as several decimetres to metres thick dykes cutting the Hamit quartz syenite and Zirattepe uralite gabbro, which is part of the CAO (Figure 3). These porphyritic dykes consist of sanidine and nosean mega- and pheno-crysts in a fine-grained matrix of plagioclase, nepheline and sanidine. Riebeckite, aegirine-augite and melanite garnet occasionally occur as phenocrysts as well as in the groundmass.

As for the structural elements of the study area, the NE-SW-, NW-SE-, N-S- and E-W-trending faults correspond in the field to crushed rocks and distinct morphological features such as offset valleys or small along-strike elongated hills. The relative displacements of the faulted blocks cannot be established. All faults cut the Mio-Pliocene Kızılırmak formation (Figure 2). Bozkurt & Mittwede (2001) and Bozkurt (2001) described neotectonic (<5 Ma) NW-SE- and NE-SW-trending faults in central Anatolia.

Analytical Techniques

Sample preparations (crushing, grinding, sieving) and heavy liquid separations to extract mafic phases (amphibole and biotite) and accessory minerals with densities $>2.90 \text{ g/cm}^3$ (zircon, titanite and apatite) were carried out at the Department of Geological Engineering, Cumhuriyet University (Sivas, Turkey).

Electron-Probe Micro-Analyses (EPMA) were performed using a Cameca Camebax instrument at the Department of Earth Sciences, University of Paris-Sud (Orsay, France); operating conditions: accelerating voltage 15 kV, current 10nA; signal integration time 10 s.

Zircon was separated using a magnetic separator and heavy liquid ($>3.3 \text{ g/cm}^3$), and then single-zircon ^{207}Pb - ^{206}Pb evaporation ages were determined at the Mineralogical Institute of the TU Bergakademie Freiberg (Germany). The analyses were carried out with a FINNIGAN MAT 262 instrument following the method described by Kober (1986, 1987).

Amphibole ^{40}Ar - ^{39}Ar dating was performed at the New Mexico Geochronology Research Laboratory (NMGRL, USA). Before irradiation, the amphiboles were purified at the NMGRL. Following irradiation, the mineral separates were step-heated using a Mo double-vacuum resistance furnace; the age spectra are based on a 12-step heating scheme; high temperature steps yielding blank argon levels were truncated. More details of the overall operation of the NMGRL can be found at internet site: <http://geoinfo.nmt.edu/publications/openfile/argon/home.html>.

Fission-track dating was performed at the Geological Institute of the TU Bergakademie Freiberg using the ζ -method (Boztug & Jonckheere 2007). The apatite mounts, covered with 50 μm uranium-free muscovite external detectors, were irradiated in the hydraulic channel of the FRM-II research reactor of the Technische Universität München (Germany). The fossil tracks were etched for 15 s in 23% HNO_3 before the irradiation; the induced tracks were etched in 40% HF for 40 min after the irradiation. The track counts were carried out in transmitted light at a magnification of 625 with an Olympus BX51 microscope using the repositioning technique (Jonckheere *et al.* 2003). The track-length measurements were carried out at a magnification of

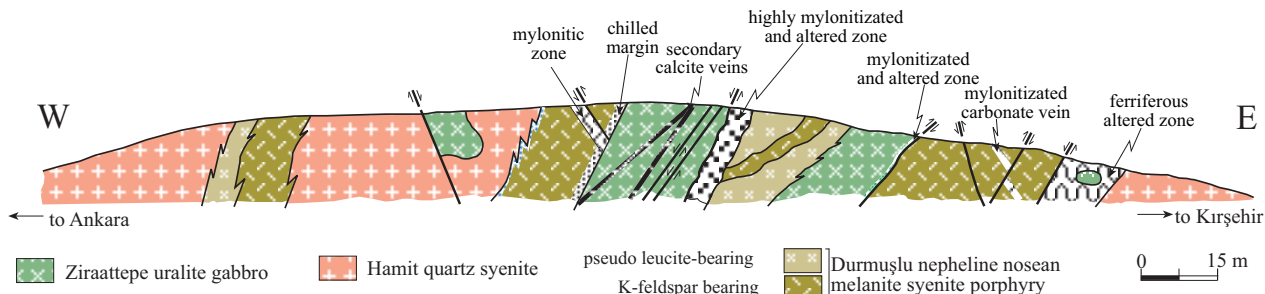


Figure 3. Geological cross section of the Durmuşlu nepheline nosean melanite syenite porphyry in a road-cut near Hamit Village.

1500 with a Zeiss Axioplan microscope equipped with an Autoscan stage and a digitiser connected to a computer with Trakscan software extended with the Easylength module. The mounts had been irradiated with 365 MeV U-ions at 15° from the normal to the surface at the GSI in Darmstadt to expose a sufficient number of confined tracks, (Jonckheere *et al.* 2007; Min *et al.* 2007). The thermal histories were modelled with HeFTy 4.0 (Ketcham 2005). The annealing equations of Laslett *et al.* (1987) were selected because no compositional information was available. Most apatite compositions are close to that of Durango ($\text{ICl-1I} \approx 0.88$) and variations within the range $0.75 < \text{ICl-1I} < 1.0$ have a modest effect on the annealing kinetics. A minimum of 50.000 candidate temperature-time T-t paths were generated at random (Monte Carlo) for each modelling run.

Analytical Results

Mineral Chemistry

The EPMA data for selected amphiboles, pyroxenes and plagioclases from the Baranadağ and Hamit units are summarized in Table 1. The mineral chemistry data were used in nomenclature of the minerals and geothermobarometrical calculations (Table 2) indicating the intrusion depths.

The amphibole structural formulae were calculated based on 23 oxygen equivalents. The resulting compositions (Table 1; Figure 4a) correspond to magmatic amphiboles (Searle & Malpas 1982) of the calcic group ($\text{Ca}_B \geq 1.50$; Leake *et al.* 1997). Al^{IV} is high in comparison with Al^{VI} in all amphiboles (Figure 4b), indicating relatively low crystallization pressures (Fleet & Barnet 1978). All Hamit and most Baranadağ amphiboles have $[\text{Na}+\text{K}]_A > 0.50$ and $\text{Ti} < 0.50$ and edenite

compositions according to their $\text{Mg}/[\text{Mg}+\text{Fe}]$ ratio and Si values (Figure 4c). Three Baranadağ amphiboles have $[\text{Na}+\text{K}]_A < 0.50$ (Figure 4d), two of magnesio-hornblende and one of ferro-actinolite composition. Figure 5a shows an Or-Ab-An diagram of the plagioclase compositions. The Hamit plagioclase ranges from andesine over oligoclase to albite (An_{42-05} ; Table 1) whereas those from Baranadağ range from andesine to oligoclase (An_{39-20} ; Table 1). The pyroxene formulae were calculated on the basis of 4 cations; the Fe^{3+} content was estimated from the charge deficit (Droop 1987). All the pyroxenes are calcic and magnesian with intermediate to limited Fe^{2+} enrichment and are classified as Si-rich and Al- and Ti-poor diopsides and hedenbergites according to Morimoto *et al.* (1988) (Table 1, Figure 5b).

Geothermobarometric Data

Geothermometric (Ti in amphibole: Anderson 1996) and geobarometric (Al in amphibole: Hammarstrom & Zen 1986 and Hollister *et al.* 1987) calculations indicate crystallization at ca. 600–685 °C and 2.5–3.2 kbar for Hamit and ca. 590–695 °C and 3.2–4.3 kbar for Baranadağ (the deviating geobarometric value (2.0 kbar) for point 27 of sample NO-171 has been excluded) (Table 2). This corresponds to intrusion depths of 8–10 km for Hamit and 10–13 km for Baranadağ, assuming a constant geobaric gradient of 0.33 kbar/km. On the other hand, these granitoid rocks cropping out in the Kaman-Kırşehir region were also studied by İlbeli (2005) with respect to geothermobarometry who has reported crystallization conditions with different temperatures, emplacement pressures and depths ranging from ca. 715 to 860 °C, from 2.6 to 5.3 kbar and from 8.7 to 18.9 km, respectively, than those of this study.

Table 1. Electron probe micro analyses (EPMA) of amphiboles, pyroxenes and plagioclases of selected rock samples from the Hamit quartz syenite and Baranadęg quartz monzonite.

AMPHIBOLE												
N° Analyse	Baranadęg											
	NO-71						NO-171					
	P 57	P 58	P 64	P 66	P 67	P 19	P 21	P 27	P 34	N° Analyse	P 3	P 9
SiO ₂	41.82	42.95	43.19	52.39	42.69	44.52	44.10	46.04	43.64	SiO ₂	44.41	44.56
TiO ₂	0.33	0.46	0.50	0.10	0.47	1.03	1.01	0.57	1.07	TiO ₂	0.73	0.81
Al ₂ O ₃	8.74	8.33	8.95	1.44	8.38	8.06	7.96	5.63	8.04	Al ₂ O ₃	7.93	7.96
FeO _t	24.42	20.21	19.51	19.56	19.03	17.61	17.31	19.30	19.58	FeO _t	16.00	17.37
MnO	0.63	0.68	0.66	0.93	0.73	0.58	0.63	0.74	0.75	MnO	0.605	0.71
MgO	6.85	9.59	10.30	10.23	10.04	11.67	11.36	10.12	9.32	MgO	12.34	11.18
CaO	11.62	11.32	11.46	12.08	11.27	11.55	11.46	11.17	10.88	CaO	11.30	11.16
Na ₂ O	1.60	1.88	1.82	0.28	1.82	1.61	1.55	1.19	1.44	Na ₂ O	2.02	2.04
K ₂ O	1.53	1.39	1.36	0.17	1.38	1.16	1.29	0.69	1.06	K ₂ O	1.31	1.21
F	0.73	1.44	1.59	0.48	1.28	0.90	0.78	0.55	0.65	F	2.04	1.57
Cl	0.30	0.08	0.11	0.03	0.07	0.07	0.08	0.07	0.11	Cl	0.07	0.07
Total	96.61	98.38	99.50	97.73	97.22	98.80	97.57	96.12	96.58	Total	98.83	98.40
Σ Ox	45.35	45.31	45.19	46.01	45.31	45.25	45.35	45.38	45.28	S Ox	45.38	45.46
Si	6.51	6.58	6.51	7.87	6.58	6.63	6.66	7.05	6.69	Si	6.67	6.75
Al IV	1.49	1.42	1.49	0.13	1.42	1.38	1.35	0.95	1.31	Al IV	1.33	1.25
T	8.00	8.00	8.00	8.00	8.00	8.00	8.00	8.00	8.00	T	8.00	8.00
Al VI	0.10	0.08	0.08	0.12	0.09	0.03	0.06	0.05	0.13	Al VI	0.06	0.10
Tl	0.03	0.05	0.05	0.01	0.05	0.11	0.11	0.06	0.12	Tl	0.08	0.08
Fe ³⁺	0.64	0.68	0.80	0.00	0.68	0.74	0.64	0.61	0.71	Fe ³⁺	0.61	0.53
Fe ²⁺	2.53	1.90	1.65	2.45	1.76	1.44	1.53	1.85	1.79	Fe ²⁺	1.39	1.66
Mn	0.08	0.08	0.08	0.11	0.09	0.07	0.08	0.09	0.09	Mn	0.07	0.09
Mg	1.59	2.18	2.31	2.29	2.3	2.58	2.55	2.3	2.12	Mg	2.76	2.52
Mg / (Mg+Fe ²⁺)	0.39	0.53	0.58	0.48	0.57	0.64	0.62	0.55	0.54	Mg	0.66	0.6
M 1-2-3	5.00	5.00	5.00	5.00	5.00	5.00	5.00	5.00	5.00	M 1-2-3	5.00	5.00
Mg	0.00	0.00	0.00	0.00	0.00	0.00	0.00	0.00	0.00	Mg	0.00	0.00
Ca	1.93	1.85	1.84	1.94	1.86	1.84	1.85	1.83	1.78	Ca	1.81	1.87
Na	0.06	0.14	0.15	0.05	0.14	0.16	0.14	0.16	0.21	Na	0.18	0.18
K	0.30	0.27	0.26	0.03	0.27	0.22	0.24	0.13	0.20	K	0.25	0.23
M 4	2.00	2.00	2.00	2.00	2.00	2.00	2.00	2.00	2.00	M 4	2.00	2.00
Na	0.42	0.41	0.38	0.02	0.40	0.30	0.18	0.21	0.20	Na	0.40	0.47
K	0.30	0.27	0.26	0.03	0.27	0.22	0.24	0.13	0.20	K	0.23	0.24
A	0.72	0.69	0.64	0.06	0.67	0.52	0.55	0.32	0.42	A	0.66	0.64
F	0.36	0.70	0.75	0.23	0.62	0.42	0.37	0.26	0.31	F	0.96	0.75
Cl	0.08	0.02	0.02	0.01	0.02	0.01	0.02	0.03	0.03	Cl	0.01	0.02
OH	1.55	1.27	1.21	1.75	1.35	1.55	1.60	1.71	1.65	OH	1.01	1.22

Table 1. (Continued)

PYROXENE									
N° Analyse	Baranadağ				Hamit				
	NO-171				NO-119				
	P 26	P 28	P 30	P 33	P 36	P 37	P 38	P 53	P 54
SiO ₂	51.342	51.078	49.017	48.981	50.742	51.659	50.733	51.341	52.074
TiO ₂	0.008	0.110	0.314	0.127	0.080	0.142	0.183	0.132	0.043
Al ₂ O ₃	0.180	1.290	2.519	0.531	0.856	1.204	1.232	1.219	0.816
FeO	12.407	11.639	15.220	14.559	12.407	11.273	11.127	12.624	12.030
MgO	9.983	11.129	9.549	9.244	10.595	11.545	11.474	10.499	10.215
MnO	1.070	0.884	0.691	1.043	0.825	0.710	0.826	0.861	0.879
CaO	23.686	22.128	20.052	22.020	22.493	22.336	22.574	23.040	22.896
K ₂ O	0.014	0.027	0.246	0.011	0.000	0.041	0.023	0.081	0.014
Na ₂ O	0.155	0.398	0.690	0.294	0.439	0.561	0.434	0.580	0.558
Cr ₂ O ₃	-	-	-	-	-	-	-	-	-
F	0.000	0.008	0.149	0.000	0.008	0.000	0.122	0.069	0.000
Cl	0.000	0.005	0.060	0.018	0.017	0.031	0.010	0.003	0.015
Total	98.845	98.696	98.507	96.828	98.462	99.502	98.738	100.448	99.540
Σ Ox	5.984	5.976	5.940	5.950	5.964	5.968	5.959	5.950	5.987
Si	1.986	1.960	1.905	1.945	1.959	1.959	1.942	1.942	1.989
Ti	0.000	0.003	0.009	0.004	0.002	0.004	0.005	0.004	0.001
Al	-	-	-	-	-	-	-	-	-
Fe	0.401	0.373	0.495	0.484	0.401	0.357	0.356	0.399	0.384
Mn	0.035	0.029	0.023	0.035	0.027	0.023	0.027	0.028	0.028
Mg	0.569	0.577	0.453	0.478	0.572	0.603	0.614	0.572	0.560
Ca	0.982	0.910	0.835	0.937	0.930	0.907	0.926	0.934	0.937
Na	0.012	0.030	0.052	0.023	0.033	0.041	0.032	0.043	0.041
Cr	-	-	-	-	-	-	-	-	-
Al IV	0.008	0.040	0.095	0.025	0.039	0.041	0.056	0.054	0.011
Al VI	0.000	0.018	0.021	0.000	0.000	0.013	0.000	0.000	0.026
Fe ³⁺	0.006	0.000	0.000	0.000	0.002	0.000	0.002	0.003	0.000
Fe ²⁺	0.395	0.373	0.495	0.484	0.399	0.357	0.354	0.396	0.384
PLAGIOLASSE									
Baranadağ									
N° Analyse	NO-71			NO-171					
	P 61	P 62	P 65	P 22	P 23	P 24			
	64.01	63.26	58.95	64.16	60.12	62.66			
SiO ₂	0.01	0.04	0.04	0.03	0.00	0.04			
TiO ₂	22.84	22.87	25.99	23.22	25.39	23.62			
Al ₂ O ₃	0.117	0.160	0.151	0.306	0.139	0.161			
MnO	0.031	0.000	0.000	0.040	0.008	0.063			
MgO	0.017	0.000	0.005	0.000	0.000	0.003			
CaO	3.961	4.016	7.551	4.035	6.778	4.760			
Na ₂ O	8.530	8.351	6.392	8.705	7.108	8.177			
K ₂ O	0.188	0.134	0.096	0.296	0.080	0.208			
BaO	-	-	-	-	-	-			
F	0.000	0.007	0.000	0.023	0.008	0.000			
Cl	0.007	0.005	0.008	0.001	0.000	0.010			
Total	99.71	98.85	99.18	100.82	99.70	99.70			
An	20.19	20.82	39.26	20.04	34.34	24.04			
Or	1.14	0.83	0.59	1.75	0.48	1.25			
Ab	78.67	78.35	60.15	78.21	65.18	74.71			

Table 1. (Continued)

N° Analyse	Hamit													
	NO-31							NO-119						
	P 4	P 5	P 10	P 12	P 14	P 15	P 16	P 42	P 43	P 45	P 47	P 48	P 49	P 51
SiO ₂	65.79	65.88	68.62	67.84	57.74	58.93	67.50	61.27	63.33	60.55	60.91	61.72	59.40	60.91
TiO ₂	0.00	0.00	0.003	0.00	0.03	0.05	0.04	0.04	0.03	0.00	0.01	0.01	0.00	0.01
Al ₂ O ₃	21.72	21.44	20.38	20.4	26.60	25.4	19.60	24.70	22.61	25.15	24.1	23.86	25.60	25.06
FeO	0.17	0.18	0.09	0.12	0.23	0.23	0.15	0.29	0.18	0.23	0.32	0.29	0.25	0.08
MnO	0.01	0.060	0.03	0.00	0.00	0.02	0.00	0.01	0.00	0.00	0.04	0.00	0.01	0.00
MgO	0.01	0.003	0.02	0.01	0.00	0.007	0.00	0.02	0.00	0.005	0.09	0.07	0.01	0.002
CaO	2.92	2.73	1.02	1.01	8.25	7.19	1.07	6.22	4.12	6.92	5.87	6.63	7.90	6.99
Na ₂ O	9.33	9.52	10.61	10.70	6.30	7.06	10.10	7.14	8.47	7.04	7.39	7.40	6.68	7.21
K ₂ O	0.62	0.54	0.17	0.04	0.16	0.18	0.21	0.33	0.20	0.14	0.29	0.17	0.19	0.18
BaO	-	-	-	-	-	-	-	-	-	-	-	-	-	-
F	0.00	0.07	0.00	0.05	0.00	0.00	0.00	0.00	0.00	0.00	0.008	0.02	0.02	0.008
Cl	0.004	0.01	0.02	0.01	0.00	0.004	0.02	0.001	0.01	0.03	0.009	0.00	0.00	0.01
Total	100.58	100.42	100.95	100.07	99.30	99.10	98.67	100.02	98.95	100.06	99.01	100.13	100.05	100.39
An	14.22	13.23	4.98	4.98	41.60	35.62	5.46	31.84	20.93	34.90	29.97	32.86	39.07	34.66
Or	3.58	3.09	0.97	0.23	0.93	1.04	1.25	2.02	1.23	0.85	1.76	1.00	1.13	0.69
Ab	82.2	83.68	94.05	94.79	54.47	63.34	93.29	66.14	77.84	64.25	68.27	66.14	59.8	64.65

Table 2. Geothermobarometric data for the Hamit quartz syenite and Baranadağ quartz monzonite. The deviating geobarometric value (2.0 kbar) for point 27 of sample NO-171 has been excluded.

Hamit: Ti in amphibole geothermometry; Al in amphibole geobarometry							
Sample	NO-31				NO-119		
Analysed point	3	9	13	19	39	41	46
Ti	0.087	0.084	0.092	0.115	0.049	0.045	0.053
Fe	2,009	2,199	1,996	2,190	2,316	2,396	2,356
Mg	2,760	2,524	2,772	2,586	2,510	2,212	2,422
Fe/(Fe+Mg)	0.421	0.466	0.419	0.459	0.480	0.520	0.493
Al	1,404	1,358	1,426	1,414	1,417	1,295	1,410
T (°C) (T < 970; T °C=(1204*Ti) +							
545 (Anderson 1996)	650	646	656	684	603	599	608
P (kb) (Hammarstrom & Zen 1986)	3.1	2.9	3.2	3.2	3.2	2.6	3.2
P (kb) (Hollister <i>et al.</i> 1987)	3.1	2.9	3.2	3.2	3.2	2.5	3.2
Baranadağ: Ti in amphibole geothermometry; Al in amphibole geobarometry							
Sample	NO-71				NO-171		
Analysed point	57	58	64	67	21	27	34
Ti	0.039	0.054	0.058	0.055	0.115	0.067	0.124
Fe	3,178	2,589	2,456	2,451	2,184	2,470	2,510
Mg	1,590	2,188	2,312	2,304	2,555	2,308	2,129
Fe/(Fe+Mg)	0.667	0.542	0.515	0.515	0.461	0.517	0.541
Al	1,604	1,504	1,588	1,522	1,416	1,017	1,452
T (°C) (T < 970; T °C=(1204*Ti) +							
545 (Anderson 1996)	592	610	614	611	683	625	694
P (kb) (Hammarstrom & Zen 1986)	4.1	3.6	4.1	3.7	3.2	1.2	3.4
P (kb) (Hollister <i>et al.</i> 1987)	4.3	3.7	4.2	3.8	3.2	1.0	3.4

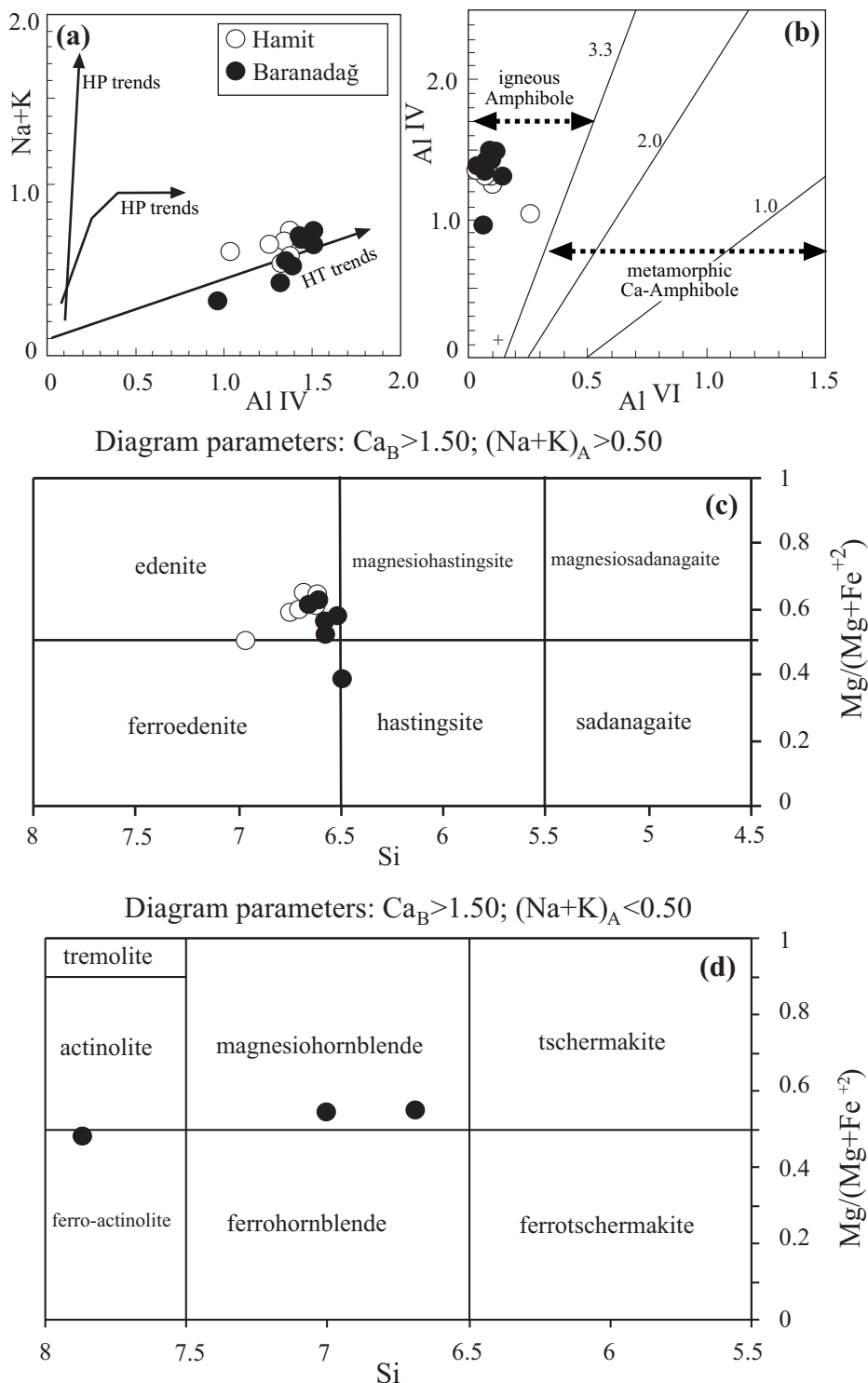


Figure 4. Chemical classification of amphiboles from the Hamit quartz syenite and Baranadağ quartz monzonite samples. (a) Plot of $[Na+K]$ vs Al^{IV} (tetrahedral) (Searle & Malpas 1982); (b) Al^{VI} (octahedral) vs Al^{IV} (tetrahedral) (Fleet & Barnett 1978); (c) plot of $Mg/(Mg+Fe^{2+})$ vs atomic Si for samples with $Ca_B > 1.5$ and $(Na+K)_A > 0.5$ (Leake *et al.* 1997); (d) plot of $Mg/(Mg+Fe^{2+})$ vs atomic Si for samples with $Ca_B > 1.5$ and $(Na+K)_A < 0.5$ (Leake *et al.* 1997). Open and filled circles stand for rock samples from the Hamit and Baranadağ units, respectively.

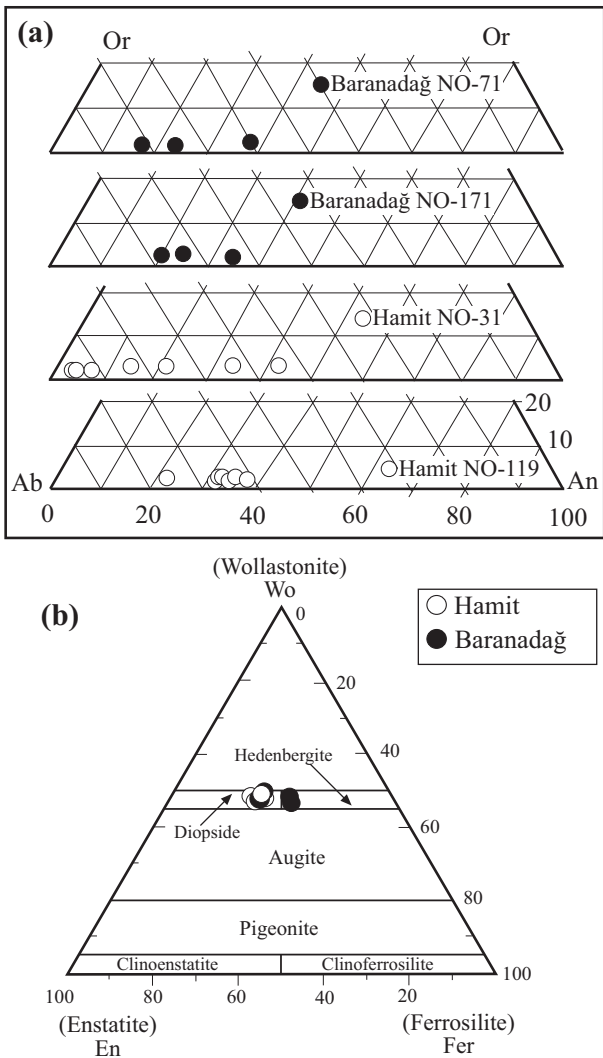


Figure 5. (a) Plagioclase compositions; (b) chemical classification (Morimoto 1988) of the pyroxenes from rock samples of the Hamit quartz syenite and Baranadağ quartz monzonite. Symbols as in Figure 4.

^{207}Pb - ^{206}Pb Zircon Ages

Table 3 reports the single-zircon ^{207}Pb - ^{206}Pb evaporation ages for the Çamsarı, Hamit and Baranadağ units. The Çamsarı sample has a weighted mean age of 95.7 ± 5.1 Ma (Figure 6a), whereas the Hamit and Baranadağ samples have weighted mean ages of 75.0 ± 11.0 Ma and 74.1 ± 4.9 Ma (Figure 6b, c). These results imply Turonian emplacement of the Çamsarı unit and Campanian emplacement of the Hamit and Baranadağ units. This is consistent with the titanite U-Pb age of 74.0 ± 2.8 Ma of Köksal *et al.* (2004) for the Baranadağ quartz monzonite

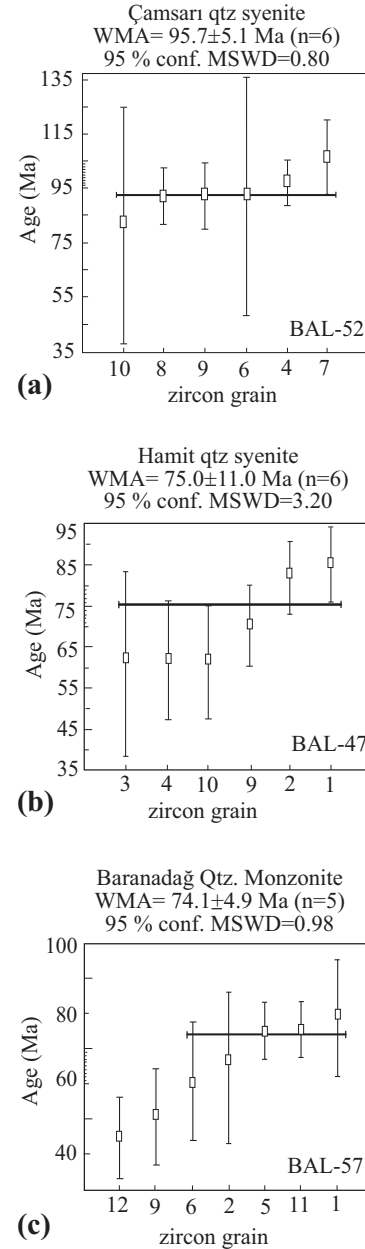


Figure 6. ^{207}Pb - ^{206}Pb single zircon evaporation ages of (a) the Çamsarı quartz syenite; (b) Hamit quartz syenite and (c) Baranadağ quartz monzonite. WMA – weighted mean age; MSWD – mean square weighted deviate.

but not with their age of 74.1 ± 0.7 Ma for the Çamsarı quartz syenite (see Discussion section).

^{40}Ar - ^{39}Ar Amphibole Ages

Table 4 presents the amphibole ^{40}Ar - ^{39}Ar ages and Figure 8 the age spectra. Samples BAL-47 and BAL-48 from

Table 3. Single-zircon $^{207}\text{Pb} / ^{206}\text{Pb}$ evaporation ages.

Granitoid	Sample-zircon No	Number of scans	$^{207}\text{Pb} / ^{206}\text{Pb}$	$^{204}\text{Pb} / ^{206}\text{Pb}$	$^{207}\text{Pb} / ^{206}\text{Pb}_{\text{corr}}$	$^{207}\text{Pb} / ^{206}\text{Pb}$	Age (Ma) (Ma+2 σ error)	Weighted mean age (Ma+2 σ error)
Hamit	BAL47-Z3	89	0.054753±0.000357	0.000523±0.0000291	0.047235±0.000341	61.1±22.4	75.0±11.0	
	BAL47-Z4	89	0.051018±0.000196	0.000273±0.0000104	0.047247±0.000183	61.7±14.4		
	BAL47-Z10	90	0.04981±0.000174	0.000188±0.00000727	0.047239±0.000172	61.3±13.9		
	BAL47-Z9	90	0.051939±0.000149	0.00032±0.00000985	0.04744±0.000121	71.4±11.3		
	BAL47-Z2	90	0.049051±0.0000734	0.000108±0.00000274	0.047645±0.0000722	81.6±8.8		
	BAL47-Z1	90	0.048812±0.0000808	0.0000874±0.00000267	0.047708±0.0000806	84.8±9.2		
Baranadağ	BAL57Z12*	89	0.052619±0.000127	0.000401±0.00000893	0.046912±0.000125	44.7±11.6	74.1±4.9	
	BAL57-Z9*	90	0.049727±0.000162	0.000196±0.0000118	0.047031±0.000167	50.8±13.7		
	BAL57-Z6	45	0.052138±0.000226	0.000348±0.0000136	0.047229±0.00023	60.8±16.8		
	BAL57-Z2	44	0.049234±0.000371	0.00015±0.0000124	0.047309±0.000325	64.8±21.5		
	BAL57-Z5	90	0.049981±0.0000615	0.00018±0.00000342	0.047524±0.00006	75.6±8.2		
	BAL57-Z15	89	0.049151±0.0000607	0.000124±0.00000233	0.047526±0.0000554	75.7±8.0		
	BAL57-Z1	36	0.05045±0.000219	0.000207±0.0000149	0.047597±0.0000229	79.2±16.6		
Çansarı	BAL52-Z1	18	0.052941±0.000684	0.000375±0.0000594	0.047639±0.000764	81.3±43.3	95.7±5.1	
	BAL52-Z8	90	0.064139±0.000113	0.00113±0.0000133	0.047849±0.000104	91.8±10.3		
	BAL52-Z9	90	0.051385±0.000138	0.000254±0.0000082	0.047851±0.000136	91.8±11.9		
	BAL52-Z6	18	0.054934±0.000691	0.000498±0.0000581	0.047852±0.000779	91.9±43.7		
	BAL52-Z4	89	0.055629±0.0000653	0.000538±0.00000548	0.047952±0.0000661	96.8±9.0		
	BAL52-Z7	89	0.055568±0.000177	0.000519±0.0000133	0.048144±0.00017	106.3±13.5		

The asterisks indicate samples that are considered as outliers and that were not included in the weighted mean age.

Table 4. ^{40}Ar - ^{39}Ar analytical data.

ID	Temp (°C)	$^{40}\text{Ar}/^{39}\text{Ar}$	$^{37}\text{Ar}/^{39}\text{Ar}$	$^{36}\text{Ar}/^{39}\text{Ar}$ (x 10 ⁻³)	$^{39}\text{Ar}_K$ (x 10 ⁻¹⁵ mol)	K/Ca	$^{40}\text{Ar}^*$ (%)	^{39}Ar (%)	Age (Ma)	$\pm 1\sigma$ (Ma)
BAL-47, Hornblende, 5.18 mg, J= 0.0036023±0.20%, D= 0.998±0.001, NM-194G, Lab#56163-01										
A	750	218.8	1.501	691.6	0.291	0.34	6.7	0.5	92	13
B	875	50.37	1.397	125.0	0.200	0.37	26.9	0.8	86.0	7.6
C	990	17.04	4.368	17.95	0.557	0.12	71.0	1.7	77.2	2.4
D	1030	12.94	4.345	6.278	6.43	0.12	88.5	12.4	73.12	0.38
E	1050	12.43	4.387	4.914	6.55	0.12	91.3	23.2	72.42	0.34
F	1070	12.43	4.111	4.237	1.27	0.12	92.7	25.4	73.5	1.0
G	1090	12.12	3.856	3.554	5.89	0.13	94.0	35.1	72.70	0.35
H	1120	11.77	3.823	2.392	22.5	0.13	96.8	72.4	72.63	0.17
I	1160	12.11	3.992	3.352	9.99	0.13	94.6	89.0	73.08	0.38
J	1220	12.59	4.193	5.350	4.78	0.12	90.3	96.9	72.55	0.56
K	1300	13.57	5.148	9.150	0.891	0.099	83.3	98.3	72.2	1.7
L	1700	22.07	15.93	41.37	0.997	0.032	50.6	100.0	71.9	1.9
Integrated age $\pm 1\sigma$		n=12		60.4	0.12		K ₂ O= 1.24%	72.90	0.25	
Plateau $\pm 1\sigma$ Steps A-L		n=12	MSWD=1.17	60.4	0.13		100.0	72.73	0.19	
ID	Temp (°C)	$^{40}\text{Ar}/^{39}\text{Ar}$	$^{37}\text{Ar}/^{39}\text{Ar}$	$^{36}\text{Ar}/^{39}\text{Ar}$ (x 10 ⁻³)	$^{39}\text{Ar}_K$ (x 10 ⁻¹⁵ mol)	K/Ca	$^{40}\text{Ar}^*$ (%)	^{39}Ar (%)	Age (Ma)	$\pm 1\sigma$ (Ma)
BAL-48, Hornblende, 4.85 mg, J= 0.0036058±0.24%, D= 0.998±0.001, NM-194G, Lab#56166-01										
xA	750	63.06	0.7441	175.8	0.714	0.69	17.7	1.0	71.2	3.6
xB	875	22.67	0.4841	42.49	0.823	1.1	44.8	2.1	64.8	2.1
xC	990	13.49	2.663	8.322	5.14	0.19	83.5	8.9	71.88	0.40
D	1030	12.10	3.319	2.894	17.8	0.15	95.3	32.6	73.65	0.21
E	1050	11.92	3.349	2.226	22.6	0.15	96.9	62.8	73.74	0.18
xF	1070	12.02	3.402	3.675	4.60	0.15	93.4	68.9	71.75	0.41
xG	1090	12.45	3.069	6.425	3.14	0.17	86.9	73.1	69.13	0.55
H	1120	12.34	3.853	3.889	2.95	0.13	93.4	77.1	73.58	0.59
I	1160	11.99	3.662	2.684	13.1	0.14	96.0	94.5	73.53	0.20
xJ	1220	11.90	3.186	3.886	3.56	0.16	92.7	99.3	70.42	0.48
xK	1300	13.21	3.395	9.584	0.540	0.15	80.8	100.0	68.2	2.7
Integrated age $\pm 1\sigma$		n=11		74.9	0.15		K ₂ O= 1.65%	72.88	0.23	
Plateau $\pm 1\sigma$ Steps D-I		n=4	MSWD=0.19	56.4	0.15		75.3	73.64	0.21	
ID	Temp (°C)	$^{40}\text{Ar}/^{39}\text{Ar}$	$^{37}\text{Ar}/^{39}\text{Ar}$	$^{36}\text{Ar}/^{39}\text{Ar}$ (x 10 ⁻³)	$^{39}\text{Ar}_K$ (x 10 ⁻¹⁵ mol)	K/Ca	$^{40}\text{Ar}^*$ (%)	^{39}Ar (%)	Age (Ma)	$\pm 1\sigma$ (Ma)
BAL-57, Hornblende, 3.87 mg, J= 0.0035909±0.16%, D= 0.998±0.001, NM-194G, Lab#56156-01										
xA	750	36.90	0.8122	118.0	0.072	0.63	5.7	0.2	13	19
xB	850	30.82	0.6560	66.53	0.266	0.78	36.4	0.7	71.2	5.7
xC	950	19.79	3.259	35.65	0.421	0.16	48.1	1.7	60.7	3.4
xD	1000	15.63	5.659	18.04	0.688	0.090	68.9	3.2	68.7	2.0
xE	1030	12.77	5.194	8.008	1.85	0.098	84.9	7.3	69.10	0.78
F	1060	12.41	4.677	5.260	6.73	0.11	90.6	22.1	71.58	0.27
G	1090	11.80	4.535	2.754	19.8	0.11	96.3	65.8	72.32	0.18
H	1120	13.59	4.949	10.68	1.44	0.10	79.8	68.9	69.10	0.95
I	1150	12.14	5.635	5.601	2.37	0.091	90.3	74.2	69.85	0.60
J	1250	12.80	5.013	6.266	11.7	0.10	88.8	100.0	72.37	0.25
Integrated age $\pm 1\sigma$		n=10		45.4	0.11		K ₂ O= 1.25%	71.58	0.21	
Plateau $\pm 1\sigma$ Steps F-J		n=5	MSWD=7.39	42.072	0.11		92.7	72.0	0.4	

Table 4. (Continued)

ID	Temp (°C)	$^{40}\text{Ar}/^{39}\text{Ar}$	$^{37}\text{Ar}/^{39}\text{Ar}$	$^{36}\text{Ar}/^{39}\text{Ar}$ ($\times 10^{-3}$)	$^{39}\text{Ar}_{\text{K}}$ ($\times 10^{-15}$ mol)	K/Ca	$^{40}\text{Ar}^*$ (%)	^{39}Ar (%)	Age (Ma)	$\pm 1\sigma$ (Ma)
BAL-61, Hornblende, 3.98 mg, J= 0.0035931±0.16%, D= 0.998±0.001, NM-194G, Lab#56155-01										
xA	700	64.30	1.872	199.2	0.506	0.27	8.7	1.1	35.9	5.2
xB	800	21.75	0.3347	38.82	0.562	1.5	47.4	2.2	65.5	2.7
xC	900	18.29	1.105	37.59	0.580	0.46	39.8	3.4	46.5	2.6
xD	1000	13.66	2.898	13.11	2.43	0.18	73.4	8.5	63.90	0.75
E	1075	11.99	4.331	4.884	25.5	0.12	91.0	61.6	69.52	0.19
F	1130	11.89	4.390	4.606	10.7	0.12	91.7	83.9	69.43	0.22
G	1150	11.86	4.812	6.782	1.40	0.11	86.5	86.8	65.44	0.90
H	1170	11.98	4.936	5.847	2.33	0.10	89.0	91.7	68.03	0.60
I	1190	12.02	4.716	4.895	2.81	0.11	91.3	97.5	69.91	0.50
J	1220	12.16	4.613	7.430	1.21	0.11	85.1	100.0	66.0	1.0
Integrated age $\pm 1\sigma$		n=10		48.1	0.12		$\text{K}_2\text{O}= 1.29\%$	68.27	0.22	
Plateau $\pm 1\sigma$ Steps E-J		n=6	MSWD=7.33	44.0	0.12		91.5	69.29	0.38	

Isotopic ratios corrected for blank, radioactive decay, and mass discrimination, not corrected for interfering reactions. Errors quoted for individual analyses include analytical error only, without interfering reaction or J uncertainties. Integrated age calculated by summing isotopic measurements of all steps. Integrated age error calculated by quadratic summation of the errors of all steps. The plateau age and associated error are the weighted means for the selected steps (Taylor 1982). Decay constants and isotopic abundances after Steiger & Jäger (1977). x symbol preceding sample ID denotes analyses excluded from plateau age calculations. Weight percent K_2O calculated from ^{39}Ar signal, sample weight, and instrument sensitivity. Ages calculated relative to FC-2 Fish Canyon Tuff sanidine inter-laboratory standard at 28.02 Ma (Renne *et al.* 1998). Decay constant: $\lambda_{\text{K}}^{\text{(total)}} = 5.543 \times 10^{-10} \text{ a}^{-1}$ (Steiger & Jäger 1977). Correction factors: $(^{39}\text{Ar}/^{37}\text{Ar})_{\text{ca}} = 0.00067 \pm 0.00005$; $(^{36}\text{Ar}/^{37}\text{Ar})_{\text{ca}} = 0.00028 \pm 0.00001$; $(^{38}\text{Ar}/^{39}\text{Ar})_{\text{K}} = 0.01077$; $(^{40}\text{Ar}/^{39}\text{Ar})_{\text{K}} = 0.01 \pm 0.002$.

Hamit give plateau ages of 72.7 ± 0.2 Ma (MSWD = 1.17; Figure 7a) and 73.6 ± 0.2 Ma (MSWD = 0.19; Figure 7b). Their total gas ages are indistinguishable at 72.9 ± 0.3 Ma and 72.9 ± 0.2 Ma. Samples BAL-57 and BAL-61 from Baranadağ give plateau ages of 72.0 ± 0.4 Ma (MSWD = 7.39; Figure 7c) and 69.3 ± 0.4 Ma (MSWD = 7.33; Figure 7d), respectively. Their total gas ages are 71.6 ± 0.2 Ma and 68.3 ± 0.2 Ma. These results show that the Hamit quartz syenite and Baranadağ quartz monzonite both cooled through the amphibole $^{40}\text{Ar}-^{39}\text{Ar}$ closure temperature (~ 500 °C; McDougall & Harrison 1999) in the Campanian to Maastrichtian.

Apatite Fission-Track Data

Table 5 reports the apatite fission-track age data of the Kaman-Kırşehir region intrusions. The age-versus-elevation plot (Figure 8) indicates rapid exhumation (> 1 km/Ma) of all the intrusive rock units (Çamsarı, Hamit, Baranadağ, Durmuşlu) during the Early to Middle Paleocene (57–61 Ma). This exhumation is confirmed by modelling of the track-length data (Figure 9). All units show fast cooling to temperatures within the ‘total stability zone’ at the beginning of their T-t histories. All samples (except one) plot in the ‘undisturbed-basement’

field in the standard-deviation versus mean-track-length plot (Gleadlow *et al.* 1986), close to the ‘volcano-type’ field (Figure 10); the Durmuşlu unit falls squarely within the ‘volcano-type’ field. Its longer mean track length is consistent with its occurrence as a typical dyke of a few metres thickness. On the other hand, Fayon *et al.* (2001) reported that the Baranadağ granitoid in the northwestern part of the CACC was exhumed during Eocene which seems to be in contradiction with our results (see Discussion section).

Discussion

Geothermochronology

Regarding the geothermochronological data, apatite fission-track ages of the Baranadağ intrusion, and the $^{207}\text{Pb}-^{206}\text{Pb}$ single-zircon evaporation age of the Çamsarı unit obtained in the present study are not in agreement with those of previous studies by Fayon *et al.* (2001) and Köksal *et al.* (2004).

The Eocene apatite fission-track age of Fayon *et al.* (2001) for Baranadağ is based on two samples (47.0 ± 6.2 and 39.2 ± 12 Ma), both of limited precision and one of which failed the χ^2 -test. On the other hand, the present

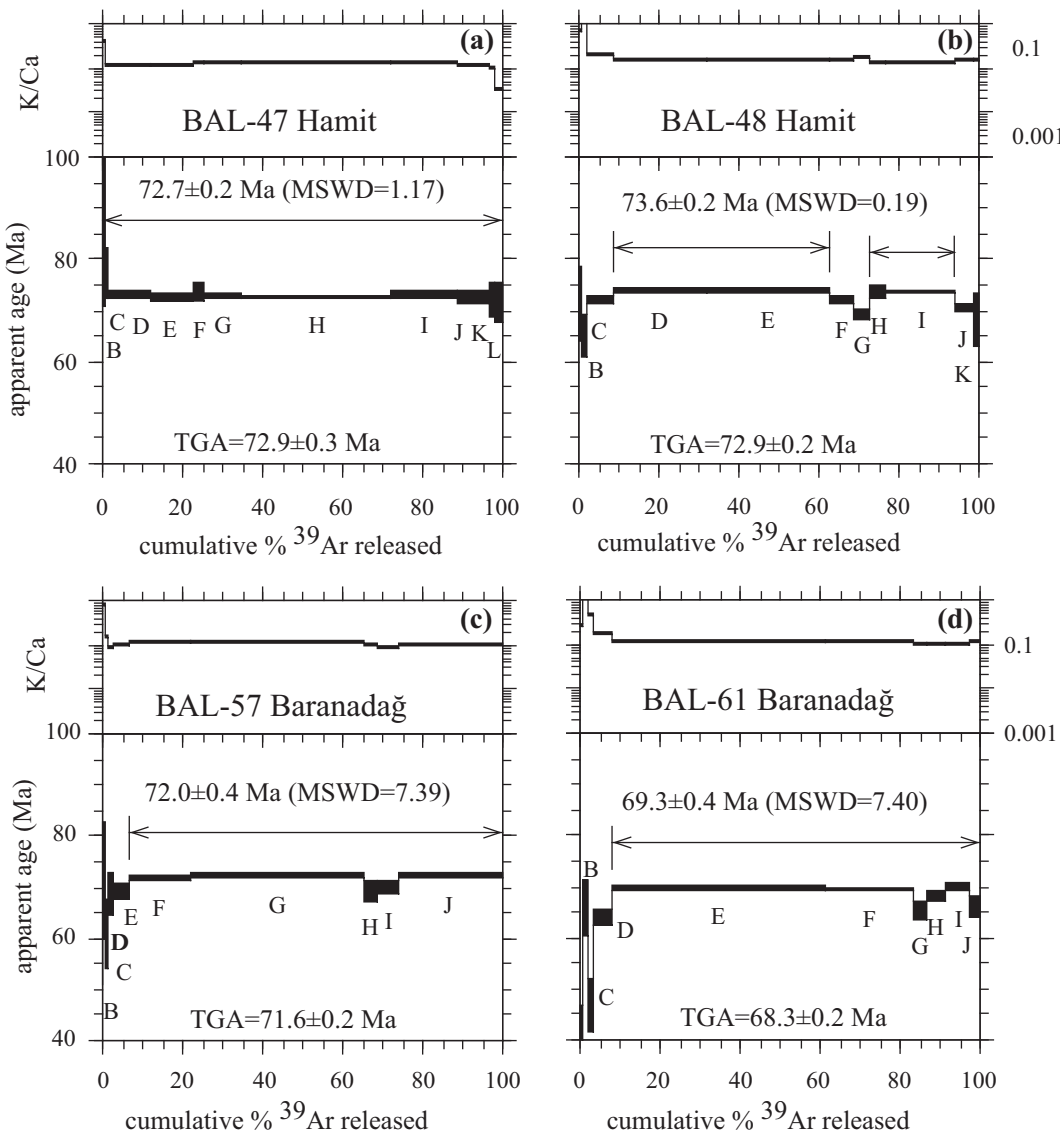


Figure 7. Amphibole ^{40}Ar - ^{39}Ar age spectra of (a, b) the Hamit quartz syenite and (c, d) Baranadağ quartz monzonite. MSWD – mean square weighted deviate; TGA – total gas age.

Paleocene apatite fission-track age for the Baranadağ unit (57.2 ± 1.8 to 60.2 ± 2.2 Ma) is consistent with those of all the other central Anatolian granitoids (Boztuğ & Jonckheere 2007).

The present ^{207}Pb - ^{206}Pb single-zircon evaporation ages are 75.0 ± 11 Ma for Hamit, 74.1 ± 4.9 Ma for Baranadağ and 95.7 ± 5.1 Ma for Çamsarı. The former are consistent with the results of Köksal *et al.* (2004), but Çamsarı appears much older than the published titanite U-Pb age (74.1 ± 0.7 Ma; Köksal *et al.* 2004). Köksal *et al.* (2006)

reported advanced metamictization of the Çamsarı zircons. Straightforward loss of radiogenic lead due to metamictization would lead to underestimate the emplacement age of the Çamsarı unit. Intense metamictization of <100 Ma zircons could, on the other hand, indicate the presence of inherited grains or much older cores, although it is unclear how these metamict zones could have survived remobilization at high temperatures. It is however a fact that Senomanian-Turonian and older crystallization ages were obtained

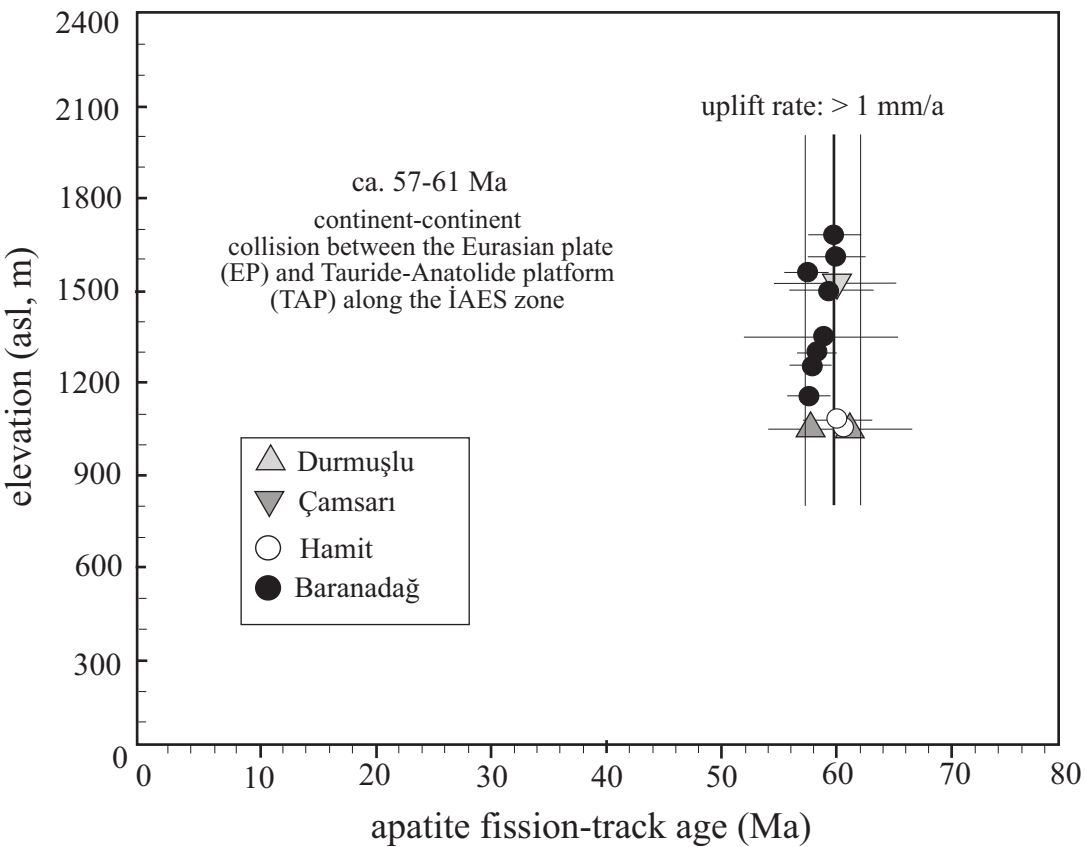


Figure 8. Apatite fission-track age vs elevation plot for the samples from the Kaman-Kirşehir region intrusions.

with different methods on other granitoid units: Üçkapılı granite (91 ± 11 Ma, Rb-Sr whole-rock isochron: Göncüoğlu 1986; 92–85 Ma, zircon U-Pb SHRIMP: Whitney *et al.* 2003), Ağaçören granitoid (110 ± 14 Ma, Rb-Sr whole-rock isochron: Güleç 1994), Murmana granitoid (110 ± 5 Ma, Rb-Sr whole-rock isochron: Zeck & Ünlü 1988). It nevertheless appears that new reliable geochronological data are needed to fix the emplacement age of the Çamsarı unit with confidence.

Geodynamic Interpretation

The closure of Neo-Tethys in the Turkish Anatolides was mainly driven by the evolution of the İzmir-Ankara-Erzincan (İAE) and Inner Tauride (IT) oceans constituting the northern branches (Şengör & Yılmaz 1981; Bozkurt & Mittwede 2001; Boztuğ & Jonckheere 2007). Most of these Neo-Tethyan oceans were proposed to begin to close in the Cenomanian–Turonian (95–90 Ma) (i.e.

Garfunkel 2004). The supra-subduction zone (SSZ) central Anatolian ophiolites (CAO) are the result of the docking of the oceanic island arc onto the TAP (Parlak & Delaloye 1999; Dilek *et al.* 1999; Floyd *et al.* 2000; Garfunkel 2004; Robertson & Ustaömer 2004; Parlak *et al.* 2006; Boztuğ & Jonckheere 2007). Following this collision between oceanic island arc and TAP, the slab break-off and/or lithospheric delamination/detachment in the Turonian–Campanian gave way an extensional post-collisional regime accompanied by medium- to high-grade metamorphism in the CACC and the emplacement of various post-collisional S-I-A-type granitoids (Boztuğ 2000; Düzgören-Aydın *et al.* 2001; Köksal *et al.* 2001, 2004; İlbeli *et al.* 2004; İlbeli 2005; Boztuğ *et al.* 2007a, b, c).

The continent-continent collision between TAP and Eurasian plate (EP) that followed the consumption of the İAE ocean is suggested to have occurred around the latest Cretaceous to Early Tertiary based mainly on structural

Table 5. Apatite fission-track data

Sample	Unit	Elevation (asl) (m)	Irradiation step	Grains	$\rho_s \pm 1\sigma$	N_s	$\rho_i \pm 1\sigma$	N_i	$P(\chi^2)$	$\rho_d \pm 1\sigma$	N_d	$\xi \text{Age} \pm 1\sigma$ (Ma)	Numb. of length	Mean track length	Stand. dev.
BAL-47	Hamit	1070	FG-01	20	1.322±0.028	2210	1.449±0.029	2423	100.00	0.423±0.003	16234	60.1±2.2	130	13.80	1.01
BAL-48	Hamit	1050	FG-01	20	0.894±0.019	2117	0.973±0.020	2304	100.00	0.423±0.003	16234	60.6±2.2	-	-	-
BAL-49	Durmüşü	1050	FG-01	11	1.857±0.115	260	2.007±0.120	281	100.00	0.423±0.003	16234	61.0±5.4	-	-	-
BAL-50	Durmüşü	1050	FG-01	10	1.217±0.071	297	1.361±0.075	332	100.00	0.423±0.003	16234	59.0±4.9	48	14.44	1.00
BAL-52	Çamşanı	1526	FG-02	03	1.100±0.068	264	1.192±0.070	286	97.86	0.416±0.003	16955	59.8±5.3	120	13.54	0.95
BAL-55	Baranadağ	1675	FG-02	20	1.422±0.034	1798	1.542±0.035	1949	100.00	0.416±0.003	16955	59.8±2.3	152	13.53	1.12
BAL-56	Baranadağ	1611	FG-02	20	0.864±0.019	2129	0.930±0.019	2291	100.00	0.416±0.003	16955	60.2±2.2	161	13.64	1.10
BAL-57	Baranadağ	1555	FG-02	20	1.095±0.019	3451	1.240±0.020	3909	99.93	0.416±0.003	16955	57.2±1.8	133	13.81	0.99
BAL-58	Baranadağ	1502	FG-02	20	1.108±0.028	1542	1.233±0.030	1716	100.00	0.416±0.003	16955	58.3±2.4	171	13.57	1.03
BAL-61	Baranadağ	1260	FG-02	20	0.621±0.015	1808	0.693±0.015	2019	100.00	0.416±0.003	16955	58.1±2.2	110	13.51	1.07
BAL-62	Baranadağ	1300	FG-02	20	1.023±0.020	2657	1.134±0.021	2945	100.00	0.416±0.003	16955	58.5±2.0	134	13.50	1.07
BAL-63	Baranadağ	1350	FG-02	06	0.991±0.031	1019	1.093±0.033	1124	99.77	0.416±0.003	16955	58.8±2.8	24	13.34	0.96
BAL-65	Baranadağ	1160	FG-02	20	1.134±0.023	2463	1.272±0.024	2762	100.00	0.416±0.003	16955	57.8±2.0	146	13.33	1.05

ρ_s = spontaneous track density (10^6 cm^{-2}), N_s = number of spontaneous tracks; ρ_i = induced track density (10^6 cm^{-2}), N_i = number of induced tracks in external detector; ρ_d = density (10^6 cm^{-3}), N_d = number of induced tracks in muscovite external detector irradiated against IRMM 540R; χ^2 value in (%); t_c (Ma)= pooled fission-track age calculated with $\xi = 313 \pm 6.1 \text{ a/cm}^2$ for IRMM 540R (Boztuğ & Jonckheere 2007); N_c = number of measured confined track lengths; L_m = mean confined track length (μm); S_{l_c} = standard deviation of the confined track length distribution (μm).

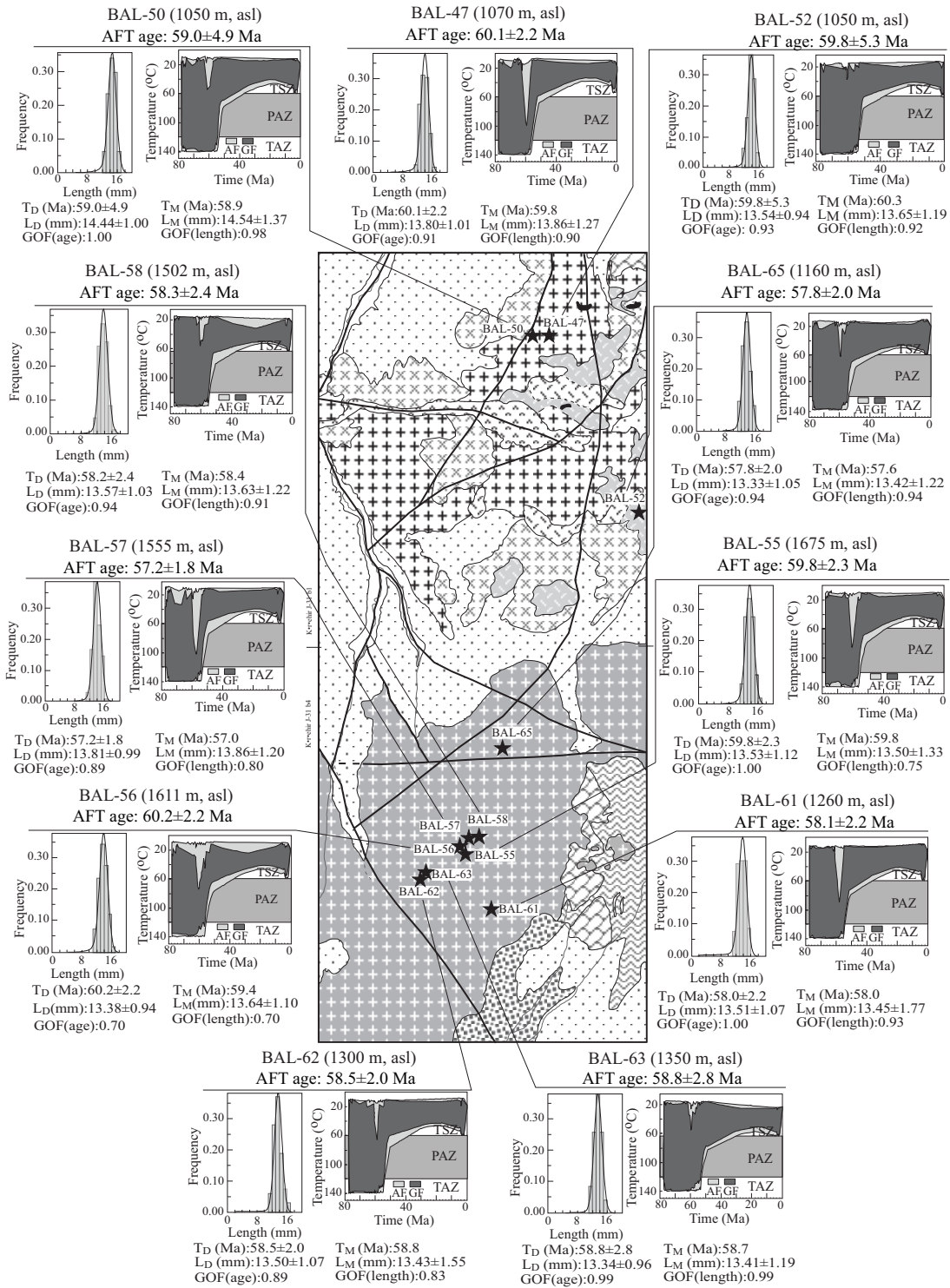


Figure 9. Modelled apatite fission-track T - t paths of the Kırşehir-Kaman region intrusions, obtained with HeFTy 4.0 (Ketcham 2005). TD—measured age, TM—model age, LD—measured mean track length, LM—model mean track length, GOF—goodness of fit, TAZ—total annealing zone; PAZ: partial annealing zone; TSZ: “total” stability zone.

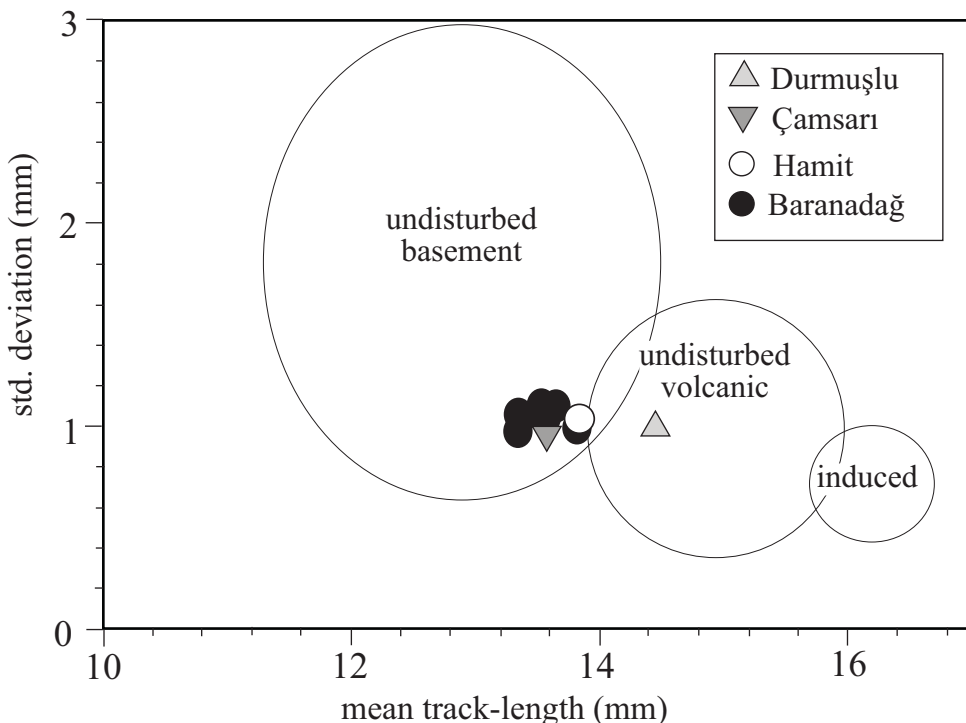


Figure 10. Plot of the standard deviation vs. the mean of the confined track length distributions (Gleadow *et al.* 1986).

data and led to crustal thickening in central Turkey (Şengör & Yılmaz 1981). A latest Cretaceous to Palaeogene compressional regime is also reported to have existed in northwest Greece and Bulgaria following the closure of the Vardar ocean, which constituted the western continuation of the İAE ocean (Burg *et al.* 1990). A most recent study by Boztuğ and Jonckheere (2007) has quantified this collision which occurred around early to middle Paleocene on the basis of apatite fission-track geothermochronology.

The close intrusion (^{206}Pb - ^{207}Pb) and cooling (^{40}Ar - ^{39}Ar) ages of the Hamit quartz syenite and Baranadağ quartz monzonite indicate either shallow-level emplacement in the crust or fairly rapid exhumation of a mid-crustal section. Otlu *et al.* (2001) reported geothermobarometric EPMA data for amphibole, plagioclase, clinopyroxene and K-feldspar minerals showing that the Baranadağ unit crystallized at P , T conditions ranging from 5.0 kbar and 680 °C (~15 km depth) to 2.0 kbar and 600 °C (~7 km depth) and the Hamit pluton solidified under conditions ranging from 4.0

kbar and 680 °C (~13 km) to 3.4 kbar and 600 °C (~11 km). The age data are thus interpreted as reflecting rapid exhumation of a mid-crustal section (Figure 11).

The Early to Middle Paleocene (57–61 Ma) fast exhumation of the Baranadağ and Hamit granitoid units is thought to result from regional compression following the collision of the EP and TAP along the İAE suture zone (Boztuğ & Jonckheere 2007). The exhumation of the granitoid and surrounding basement rocks was accompanied by the development of peripheral foreland basins or piggy-back basins (Görür *et al.* 1998; Gürer & Aldanmaz 2002) containing Upper Paleocene to Lower/Middle Eocene conglomerates and flysch-type sediments. Fast erosional balancing of the accelerated uplift sustained the rapid infilling of these basins. The faults accommodating the Early to Middle Paleocene compressional tectonics in central Anatolia have not been identified in the field; it is however possible that they are hidden by the sedimentary and volcanic cover.

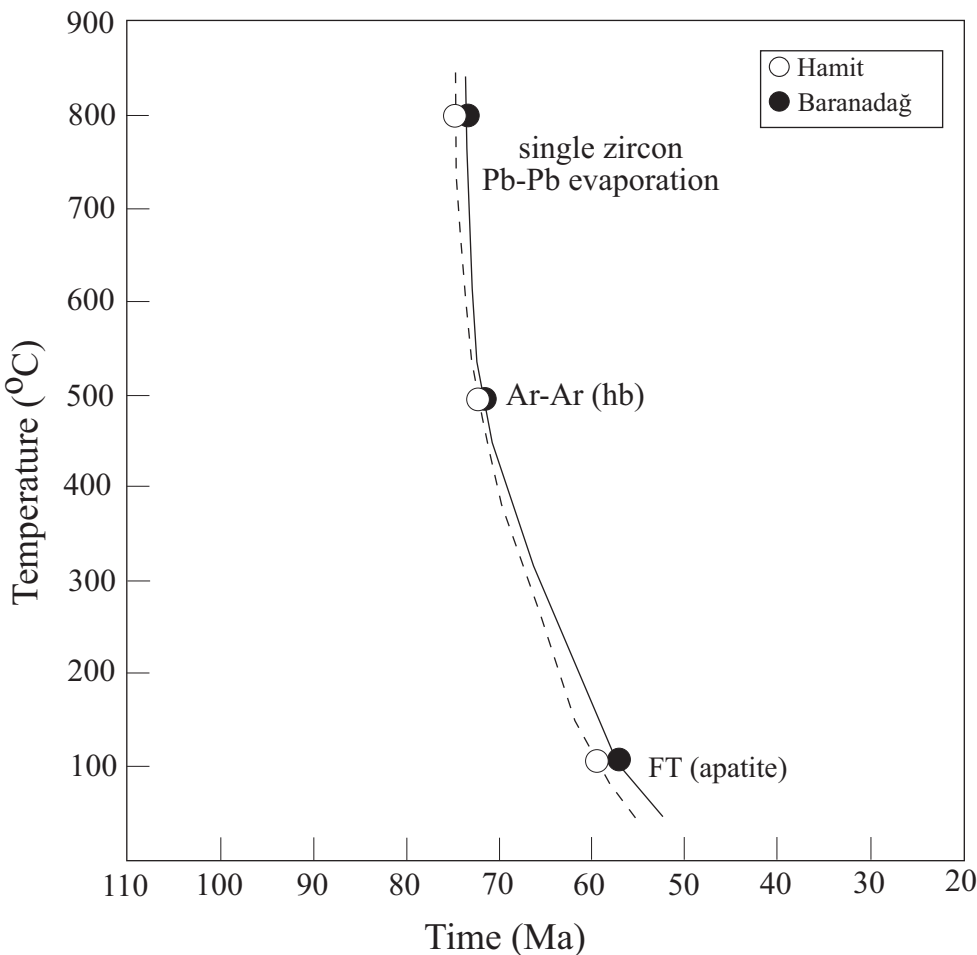


Figure 11. Cooling curve of the Hamit quartz syenite and Baranadağ quartz monzonite based on the age (Ma) and closure temperatures of different geochronological dating methods. The closure temperatures of ^{206}Pb - ^{207}Pb single zircon evaporation, amphibole ^{40}Ar - ^{39}Ar and apatite fission-track methods are assigned as 750–800 °C (Lee *et al.* 1997; Cherniak & Watson 2000), 500 °C (McDougall & Harrison 1999) and 120 °C (Wagner & Van den Haute 1992; Wagner 1998), respectively.

Conclusions

Integrated geothermochronology data consisting of ^{207}Pb - ^{206}Pb single zircon evaporation ages, amphibole ^{40}Ar - ^{39}Ar ages and apatite fission-track dating provide a wide age spectra ranging from emplacement through cooling to exhumation for the Kaman-Kırşehir region intrusions which were crystallized at the mid-crustal depths in central Anatolia, Turkey. ^{207}Pb - ^{206}Pb single zircon evaporation ages yield an emplacement age of 95.7 ± 5.1 Ma for the Çamsarı quartz syenite, 75.0 ± 11.0 Ma for the Hamit quartz syenite and 74.1 ± 4.9 Ma for the Baranadağ quartz monzonite. Amphibole ^{40}Ar - ^{39}Ar ages reveal a

cooling age of ca. 73 Ma for both of the Hamit and Baranadağ units. Apatite fission-track geothermochronology, comprising dating and track-length data, determine an exhumation history for the Kaman-Kırşehir region intrusions which reveals a rapid tectonic unroofing with an uplift rate > 1 mm/a that occurred 57–61 Ma ago. The Early–Middle Paleocene fast exhumation of Kaman-Kırşehir region intrusions is considered to be resulted from a compressional regime, instituted after the continent-continent collision between the TAP and EP along the İAE suture zone, following the consumption of the İAE ocean. The resulting rapid

tectonic exhumation along thrust faults also triggered the formation of the central Anatolian peripheral foreland basins.

Acknowledgement

This research was supported by TÜBİTAK-Ankara (102 Y 149) and the Cumhuriyet University Research Foundation (CÜBAP-M 255) in Sivas. Prof. D. Boztuğ is indebted to TÜBİTAK-BAYG, DFG and DAAD for grants to work at the Fission-Track Laboratory of TU Bergakademie Freiberg, Sachsen, Germany. R. Jonckheere is indebted to the German Science Foundation (DFG) for financial support under grant Ra 440/26. R.A. Ketcham (University of Texas at Austin) has supplied the HeFTy 4.0 software for thermal history modelling. B. Bonin and B. Platevoet

(University of Paris Sud, Orsay, France) have helped us for EPMA of rock samples. L. Ratschbacher (TU Bergakademie Freiberg) is kindly thanked for his helpful discussion on the manuscript. The authors are pleased to acknowledge their debt to H. Gerstenberg (Forschungsneutronenquelle Heinz Maier-Leibnitz) and Lin Xilei (Radiochemie) of the TU München for the thermal neutron irradiations and neutron fluence measurements. We thank to Greg B. Arehart (University Nevada Reno, USA) and Serhat Köksal (METU, Ankara, Turkey) for their reviews and helpful comments which improved the manuscript. Fatma Toksoy Köksal is kindly thanked for re-calculation and correction of the geothermobarometry data. Nilgün Güleç and Erdin Bozkurt (METU, Ankara, Turkey) are kindly thanked for their efforts during editorial handling.

References

- AKIMAN, O., ERLER, A., GÖNCÜOĞLU, M.C., GÜLEÇ, N., GEVEN, A., TÜRELİ, T.K. & KADIOĞLU, Y.K. 1993. Geochemical characteristics of granitoids along the western margin of the Central Anatolian Crystalline Complex and their tectonic implications. *Geological Journal* **28**, 371–382.
- ANDERSON, J.L. 1996. Status of thermobarometry in granitic batholiths. *Transactions of the Royal Society of Edinburgh: Earth Sciences* **87**, 125–138.
- ATAMAN, G. 1972. Ankara'nın güneydoğusundaki granitik-granodioritik kütlelerden Cefalik Dağın radyometrik yaşı hakkında ön çalışma [The preliminary study on the radiometric age of Cefalik Dağı that is one of the granitic-granodioritic bodies in the SW of Ankara]. *Hacettepe Fen ve Mühendislik Bilimleri Dergisi* **2**, 44–49 [in Turkish with English abstract].
- BOZKURT, E. 2001. Neotectonics of Turkey—a synthesis. *Geodinamica Acta* **14**, 3–30.
- BOZKURT, E. & MITTWEDE, S.K. 2001. Introduction to the geology of Turkey: a synthesis. *International Geology Review* **43**, 578–594.
- BOZTUĞ, D. 1998. Post-collisional Central Anatolian alkaline plutonism, Turkey. *Turkish Journal of Earth Sciences* **7**, 145–165.
- BOZTUĞ, D. 2000. S-I-A-type intrusive associations: geodynamic significance of synchronism between metamorphism and magmatism in Central Anatolia, Turkey. In: Bozkurt, E., WINCHESTER, J.A. & PIPER, J.D.A. (eds), *Tectonics and Magmatism in Turkey and the Surrounding Area*. Geological Society, London, Special Publications **173**, 407–424.
- BOZTUĞ, D. & AREHART, G.B. 2007. Oxygen and sulfur isotope geochemistry revealing a significant crustal signature in the genesis of the post-collisional granitoids in central Anatolia, Turkey. *Journal of Asian Earth Sciences* **30**, 403–416.
- BOZTUĞ, D., AREHART, G.B., PLATEVOET, B., HARLAVAN, Y. & BONIN, B. 2007c. High-K calc-alkaline I-type granitoids from the composite Yozgat batholith generated in a post-collisional setting following continent-oceanic island arc collision in central Anatolia, Turkey. *Mineralogy and Petrology* **91**, 191–223.
- BOZTUĞ, D. & HARLAVAN, Y. 2008. K-Ar ages of granitoids unravel the stages of Neo-Tethyan convergence in the eastern Pontides and central Anatolia, Turkey. *International Journal of Earth Sciences* **97**, 585–599.
- BOZTUĞ, D., HARLAVAN, Y., AREHART, G.B., SATIR, M. & AVCI, N. 2007a. K-Ar age, whole-rock and isotope geochemistry of A-type granitoids in the Divrigi-Sivas region, eastern-central Anatolia, Turkey. *Lithos* **97**, 193–218.
- BOZTUĞ, D. & JONCKHEERE, R.C. 2007. Apatite fission-track data from central Anatolian granitoids (Turkey) constrain Neo-Tethyan closure. *Tectonics* **26**, TC3011, doi:10.1029/2006TC001988.
- BOZTUĞ, D., TICHOMIROWA, M. & BOMBACH, K. 2007b. ^{207}Pb - ^{206}Pb single-zircon evaporation ages of some granitoid rocks reveal continent-oceanic island arc collision during the Cretaceous geodynamic evolution of the central Anatolian crust, Turkey. *Journal of Asian Earth Sciences* **31**, 71–86.
- BURG, J.P., IVANOV, Z., RICOU, L.E., DIMOV, D. & KLAIN, L. 1990. Implications of shear-sense criteria for the tectonic evolution of the Central Rhodope Massif, southern Bulgaria. *Geology* **18**, 451–454.
- CHERNIAK, D.J. & WATSON, E.B. 2000. Pb diffusion in zircon. *Chemical Geology* **172**, 5–24.
- DILEK, Y., THY, P., HACKER, B. & GRUNDVIG, S. 1999. Structure and petrology of Tauride ophiolites and mafic dike intrusions (Turkey): implications for the Neotethyan Ocean. *Geological Society of America Bulletin* **111**, 1192–1216.

- DODSON, M.H. 1973. Closure temperature in cooling geochronological and petrological systems. *Contributions to Mineralogy and Petrology* **40**, 259–274.
- DODSON, M.H. 1979. Theory of cooling ages. In: JÄGER, E. & HUNZIKER, J.C. (eds), *Lectures on Isotope Geology*. Springer Verlag, Berlin, 194–202.
- DROOP, G.T.R. 1987. A general equation for estimating Fe^{3+} concentrations in ferromagnesian silicates and oxides from microprobe analyses, using stoichiometric criteria. *Mineralogical Magazine* **51**, 431–435.
- DÜZGÖREN-AYDIN, N., MALPAS, W., GÖNCÜOĞLU, M.C. & ERLER, A. 2001. Post collisional magmatism in Central Anatolia, Turkey: field, petrographic and geochemical constraints. *International Geology Review* **43**, 695–710.
- ERLER, A. & GÖNCÜOĞLU, M.C. 1996. Geologic and tectonic setting of the Yozgat batholith, Northern Central Anatolian Crystalline Complex, Turkey. *International Geology Review* **38**, 714–726.
- FAYON, A.K. & WHITNEY, D. L. 2007. Interpretation of tectonic versus magmatic processes for resetting apatite fission track ages in the Niğde Massif, Turkey. *Tectonophysics* **434**, 1–13.
- FAYON, A.K., WHITNEY, D.L., TEYSSIER, C., GARVER, J.I. & DILEK, Y. 2001. Effects of plate convergence obliquity on timing and mechanisms of exhumation of a mid-crustal terrain, the Central Anatolian Crystalline Complex. *Earth and Planetary Science Letters* **192**, 191–205.
- FLEET, M.E. & BARNETT, R.L. 1978. $\text{Al}^{\text{IV}}/\text{Al}^{\text{VI}}$ partitioning in calciferous amphiboles from the Frood mine, Sudbury, Ontario. *Canadian Mineralogist* **16**, 527–532.
- FLOYD, P.A., GÖNCÜOĞLU, M.C., WINCHESTER, J.A. & YALINIZ, M.K. 2000. Geochemical character and tectonic environment of Neotethyan Ophiolitic fragments and metabasites in the Central Anatolian Crystalline Complex, Turkey. In: BOZKURT, E., WINCHESTER, J.A. & PIPER, J.D.A. (eds), *Tectonics and Magmatism in Turkey and the Surrounding Area*. Geological Society, London, Special Publications **173**, 183–202.
- GARFUNKEL, Z. 2004. Origin of the Eastern Mediterranean basin: a re-evaluation. *Tectonophysics* **391**, 11–34.
- GLEADOW, A.J.W., DUDDY, I.R., GREEN, P.F. & LOVERING, J.F. 1986. Confined fission track lengths in apatite: a diagnostic tool for thermal history analysis. *Contributions to Mineralogy and Petrology* **94**, 405–415.
- GÖNCÜOĞLU, M.C. 1986. Geochronological data from the southern part (Niğde area) of the Central Anatolian Massif. *Bulletin of Mineral Research and Exploration Institute (MTA) of Turkey* **105/106**, 83–96.
- GÖRÜR, N., TÜYSÜZ, O. & ŞENGÖR, A.M.C. 1998. Tectonic evolution of the central Anatolian basins. *International Geology Review* **40**, 831–850.
- GÜLEÇ, N. 1994. Rb-Sr isotope data from the Ağaçören Granitoid (East of Tuz Gölü): Geochronological and genetical implications. *Turkish Journal of Earth Sciences* **3**, 39–43.
- GÜndođu, M.N., BROs, R., KURUÇ, A. & BAYHAN, H. 1988. Rb-Sr whole-rock systematic of the Bayındır feldspathoidal syenites (Kaman-Kirşehir). *Symposium for the 20th Anniversary of Earth Sciences at Hacettepe University, October 25–27, Abstracts*, p. 55.
- GÜRER, O.F. & ALDANMAZ, E. 2002. Origin of the Upper Cretaceous-Tertiary sedimentary basins within the Tauride-Anatolide platform in Turkey. *Geological Magazine* **139**, 191–197.
- HAMMARSTROM, J.M. & ZEN, E-AN. 1986. Aluminum in hornblende: an empirical igneous barometer. *American Mineralogist* **71**, 1297–1313.
- HOLLISTER, L.S., GRISOM, G.C., PETERS, E.K., STOWELL, H.H. & SISSON, V.B. 1987. Confirmation of the empirical correlation of Al in hornblende with pressure of solidification of calc-alkaline plutons. *American Mineralogist* **72**, 231–239.
- İLBİEYLİ, N. 2005. Mineralogical-geochemical constrains on intrusives in central Anatolia, Turkey: tectono-magmatic evolution and characteristics of mantle source. *Geological Magazine* **142**, 187–207.
- İLBİEYLİ, N., PEARCE, J.A., THIRWALL, M.F. & MITCHELL, J.G. 2004. Petrogenesis of collision-related plutons in central Anatolia, Turkey. *Lithos* **72**, 163–182.
- JONCKHEERE, R.C., RATSCHBACHER, L. & WAGNER, G.A. 2003. A repositioning technique for counting induced fission tracks in muscovite external detectors in single-grain dating of minerals with low and inhomogeneous uranium concentrations. *Radiation Measurements* **37**, 217–219.
- JONCKHEERE, R.C., ENKELMANN, E., MIN, M., TRAUTMANN, C. & RATSCHBACHER, L. 2007. Improved confined fission-track length measurements in apatite using ion irradiation and step etching. *Chemical Geology* **242**, 202–217.
- KADIOĞLU, Y.K., DILEK, Y., GÜLEÇ, N. & FOLAND, K.A. 2003. Tectonomagmatic evolution of bimodal plutons in the Central Anatolian Crystalline Complex, Turkey. *Journal of Geology* **111**, 671–690.
- KADIOĞLU, Y.K., DILEK, Y. & FOLAND, K.A. 2006. Slab break-off and synollisional origin of the Late Cretaceous magmatism in the Central Anatolian crystalline complex, Turkey. In: DILEK, Y. & PAVLIDES, S. (eds), *Postcollisional Tectonics and Magmatism in the Mediterranean Region and Asia*. Geological Society of America, Special Paper **409**, 381–415.
- KETCHAM, R.A. 2005. Forward and inverse modeling of low-temperature thermochronometry data. *Reviews in Mineralogy and Geochemistry* **58**, 275–314.
- KOBER, B. 1986. Whole-grain evaporation for $^{207}\text{Pb}/^{206}\text{Pb}$ -age investigations on single zircons using a double-filament thermal ion source. *Contributions to Mineralogy and Petrology* **93**, 482–490.
- KOBER, B. 1987. Single-zircon evaporation combined with Pb+ emitter bedding for $^{207}\text{Pb}/^{206}\text{Pb}$ -age investigations using thermal ion mass spectrometry, and implications to zirconology. *Contributions to Mineralogy and Petrology* **96**, 63–71.

- KÖKSAL, S. & GÖNCÜOĞLU, M.C. 2008. Sr and Nd isotopic characteristics of some S-, I- and A-type granitoids from central Anatolia. *Turkish Journal of Earth Sciences* **17**, 111–127.
- KÖKSAL, S., GÖNCÜOĞLU, M.C. & FLOYD, P.A. 2001. Extrusive members of post collisional A-type magmatism in Central Anatolia: Karahıdır Volcanics, İdış Dağı-Avanos area, Turkey. *International Geology Review* **43**, 683–694.
- KÖKSAL, S., ROMER, R.L., GÖNCÜOĞLU, M.C. & TOKSOY-KÖKSAL, F. 2004. Timing of post-collision H-type to A-type granitic magmatism: U-Pb titanite ages from the Alpine central Anatolian granitoids Turkey. *International Journal of Earth Sciences* **93**, 974–989.
- KÖKSAL, S., TOKSOY-KÖKSAL, F. & GÖNCÜOĞLU, M.C. 2006. Zircon growth in distinct granitoid types: examples from Central Anatolian Granitoids. *59th Geological Congress of Turkey, Ankara, Abstracts*, 271–272.
- KURUÇ, A. 1990. *Rb-Sr Geochemistry of Syenitoids from Kaman-Kırşehir Region*. MSc Thesis, Hacettepe University [in Turkish with English abstract, unpublished].
- LASLETT, G.M., GREEN, P.E., DUDDY, I.R. & GLEADOW, A.J.W. 1987. Thermal annealing of fission tracks in apatite. 2. A quantitative analysis. *Chemical Geology* **65**, 1–13.
- LEAKE, B.E., WOOLEY, A.R., ARPS, C.E.S., BIRCH, W.D., GILBERT, M.C., GRICE, J.D., HAWTHORNE, F.C., KATO, A., KISCH, H.J., KRIVOVICHÉV, V.G., LINTHOUT, K., LAIRD, J., MANDARINO, J.A., MARESCH, W.V., NICKEL, E.H., ROCK, N.M.S., SCHUMACHER, J.C., SMITH, D.C., STEPHENSON, N.C.N., UNGARETTI, L., WHITTAKER, E.J.W. & YOUNGHUI, G. 1997. Nomenclature of amphiboles: report of the subcommittee on amphiboles of the International Mineralogical Association, Commission on New Minerals and Mineral Names. *American Mineralogist* **82**, 1019–1037.
- LEE, J.K.W., WILLIAMS, I.S. & ELLIS, D.J. 1997. Pb, U and Th diffusion in natural zircon. *Nature* **390**, 15–162.
- MCDougall, I. & HARRISON, T.M. 1999. *Geochronology and Thermochronology by the $^{40}\text{Ar}/^{39}\text{Ar}$ Method*. Oxford University Press.
- MIN, M., ENKELMANN, E., JONCKHEERE, R.C., TRAUTMANN, C. & ATSCHBACHER, L. 2007. Measurements of fossil confined fission tracks in ion-irradiated geological apatite samples with low track densities. *Nuclear Instruments and Methods in Physics Research Section B: Beam Interactions with Materials and Atoms* **259**, 943–950.
- MORIMOTO, N., FABRIES, J., FERGUSON, A.K., GINZBURG, I.V., ROSS, M., SEIFFERT, F.A., ZUSSMAN, J., AOKI, K. & GOTTAUDI, G. 1988. Nomenclature of pyroxenes. *Contributions to Mineralogy and Petrology* **99**, 55–76.
- OKAY, A.İ. & TÜYSÜZ, O. 1999. Tethyan Sutures Of Northern Turkey. In: DURAND, B., JOLIVET, L., HORVATH, F. & SERANNE, M. (eds), *The Mediterranean Basins: Tertiary Extension within the Alpine Orogen*. Geological Society, London, Special Publications **156**, 475–515.
- OTLU, N. & BOZTUĞ, D. 1998. The coexistence of the silica oversaturated (ALKOS) and undersaturated alkaline (ALKUS) rocks in the Kortundağ and Baranadağ plutons from the Central Anatolian alkaline plutonism, E Kaman/NW Kırşehir, Turkey. *Turkish Journal of Earth Sciences* **7**, 241–257.
- OTLU, N., BOZTUĞ, D. & BONIN, B., 2001. Mineral chemistry and geothermobarometry of some silica oversaturated alkaline plutons from the post-collisional alkaline plutonism in Central Anatolia, Turkey. *Fourth International Turkish Geology Symposium, (ITGS-IV), 24–28 September 2001, Abstracts*, p. 56.
- ÖNAL, A., BOZTUĞ, D., KÜRÜM, S., HARLAVAN, Y., AREHART, G.B. & ARSLAN, M. 2005. K-Ar age determination, whole rock and oxygen isotope geochemistry of the post-collisional Bizmişen and Çaltı plutons, SW Erzincan, eastern Central Anatolia, Turkey. *Geological Journal* **40**, 457–476.
- PARLAK, O. & DELALOYE, M. 1999. Precise $^{40}\text{Ar}/^{39}\text{Ar}$ ages from the metamorphic sole of the Mersin ophiolite (southern Turkey). *Tectonophysics* **301**, 145–158.
- PARLAK, O., YILMAZ, H. & BOZTUĞ, D. 2006. Origin and tectonic significance of the metamorphic sole and isolated dykes of the Divriği Ophiolite (Sivas, Turkey): Evidence for slab break-off prior to ophiolite emplacement. *Turkish Journal of Earth Sciences* **15**, 25–45.
- RENNE, P.R., SWISHER, C.C., DEINO, A.L., KARNER, D.B., OWENS, T.L. & DE PAOLO, D.J. 1998. Intercalibration of standards, absolute ages and uncertainties in $^{40}\text{Ar}/^{39}\text{Ar}$ dating. *Chemical Geology* **145**, 117–152.
- ROBERTSON, A.H.F. & USTAÖMER, T. 2004. Tectonic evolution of the Intra-Pontide suture zone in the Armutlu Peninsula, NW Turkey. *Tectonophysics* **381**, 175–209.
- SEARLE, M.P. & MALPAS, J. 1982. Petrochemistry and origin of subophiolitic metamorphic and related rocks in the Oman Mountains. *Journal of the Geological Society, London* **139**, 235–248.
- ŞENGÖR, A.M.C. & YILMAZ, Y. 1981. Tethyan evolution of Turkey: a plate tectonic approach. *Tectonophysics* **75**, 181–241.
- STEIGER, R. H. & JÄGER, E. 1977. Subcommission on geochronology: convention on the use of decay constants in geo- and cosmochronology. *Earth and Planetary Science Letters* **36**, 359–363.
- TATAR, S. & BOZTUĞ, D. 2005. The syn-collisional Danaciobaşı biotite leucogranite derived from the crustal thickening in central Anatolia (Kırıkkale), Turkey. *Geological Journal* **40**, 571–591.
- TAYLOR, J.R. 1982. *An Introduction to Error Analysis: The Study of Uncertainties in Physical Measurements*. University Science Books, Mill Valley, California.
- WAGNER, G.A. 1998. *Age Determination of Young Rocks and Artifacts. Physical and Chemical Clocks in Quaternary Geology and Archaeology*. Springer, Heidelberg.
- WAGNER, G.A. & VAN DEN HAUTE, P. 1992. *Fission Track Dating*. Ferdinand Enke Verlag Stuttgart, Kluwer Academic, Dordrecht.
- WHITNEY, D.L. & HAMILTON, M.A. 2004. Timing of high grade metamorphism in central Turkey and the assembly of Anatolia. *Journal of the Geological Society, London* **161**, 823–828.
- WHITNEY, D.L., TEYSSIER, C., DILEK, Y. & FAYON, A.K. 2001. Metamorphism of the Central Anatolian Crystalline Complex, Turkey: influence of orogen-normal collision vs. wrench dominated tectonics on P-T-t paths. *Journal of Metamorphic Geology* **19**, 411–432.

- WHITNEY, D.L., TEYSSIER, C., FAYON, A.K., HAMILTON, M.A. & HEIZLER, M. 2003. Tectonic controls on metamorphism, partial melting, and intrusion: timing and duration of regional metamorphism and magmatism in the Niğde Masif, Turkey. *Tectonophysics* **376**, 37–60.
- YALINIZ, M.K., AYDIN, N.S., GÖNCÜOĞLU, M.C. & PARLAK, O. 1999. Terlemez quartz monzonite of central Anatolia (Aksaray-Sarıkaman): age, petrogenesis and geotectonic implications for ophiolite emplacement. *Geological Journal* **34**, 233–242.
- YALINIZ, K.M., FLOYD, P. & GÖNCÜOĞLU, M.C. 1996. Suprasubduction zone ophiolites of Central Anatolia: geochemical evidence from the Sarıkaman ophiolite, Aksaray, Turkey. *Mineralogical Magazine* **60**, 697–710.
- YALINIZ, K.M., FLOYD, P. & GÖNCÜOĞLU, M.C. 2000. Geochemistry of volcanic rocks from Çiçekdağ ophiolite, central Anatolia, Turkey, and their inferred tectonic setting within the northern branch of Neotethyan ocean. In: BOZKURT, E., WINCHESTER, J.A. & PIPER, J.D.A. (eds). *Tectonics and Magmatism in Turkey and the Surrounding Area*. Geological Society, London, Special Publications **173**, 203–218.
- ZECK, H.P. & ÜNLÜ, T. 1988. Alpine ophiolite obduction before 110 ± 5 Ma ago, Taurus belt, Eastern central Turkey. *Tectonophysics* **145**, 55–62.